APPENDIX 2.10.3

TABLE OF CONTENTS

Page

2.10.3 NUHOMS®-61BT DSC (CANISTER AND BASKET) STRUCTURAL EVALUATION 2.10.3-1

2.10.3.1 Introduction 2.10.3-1
2.10.3.2 Fuel Basket Structural Analysis 2.10.3-2
2.10.3.3 Canister Structural Analysis 2.10.3-31
2.10.3.4 References 2.10.3-47

LIST OF TABLES

2.10.3-1 Temperature Dependent Material Properties
2.10.3-2 Summary of Basket Normal Condition Stress Analysis
2.10.3-3 Summary of Basket Accident Condition Stress Analysis
2.10.3-4 Summary of Hold Down Ring Accident Condition Stress Analysis
2.10.3-5 Summary of Loads Used for Different Drop Orientations
2.10.3-6 Summary of Canister Normal Condition Stress Analysis
2.10.3-7 Summary of Canister Accident Condition Stress Analysis

LIST OF FIGURES

2.10.3-1 Basket Cross Section Finite Element Model
2.10.3-2 Basket Cross Section Finite Element Model – Fuel Compartments
2.10.3-3 Basket Cross Section Finite Element Model – Outer Wrap
2.10.3-4 Basket Cross Section Finite Element Model – Support Rails
2.10.3-5 Basket Side Drop Orientations
2.10.3-6 Gap Sizes between Basket Rails and Canister Inner Surface
2.10.3-7 Gap Sizes between Canister Outer Surface and Transport Cask Inner Surface
2.10.3-8 Finite Element Model – Canister & Gap Elements
2.10.3-9 Finite Element Model – Canister & Gap Elements, Enlarged View
2.10.3-10 Basket Temperature Distribution at the Middle Section
2.10.3-11 Basket Temperature Distribution at the Top Section
2.10.3-12 Basket Temperature Distribution at the Bottom Section
2.10.3-13 Basket ¼ Section Finite Element Model for Thermal Stress Analysis
2.10.3-14 Basket ¼ Section Finite Element with Nodal Couplings and Boundary Conditions
2.10.3-15 Thermal Stress Analysis Geometry
2.10.3-16 Support Rail Temperature Distribution at the Middle Section
2.10.3-17 Support Rail Temperature Distribution at the Top Section
2.10.3-18 Support Rail Temperature Distribution at the Bottom Section
2.10.3-19 Basket Rail Type 1 Finite Element Model
2.10.3-20 Basket Rail Type 2 Finite Element Model
2.10.3-21 45^0 Orientation Side Drop – Loading Condition
2.10.3-22 60^0 Orientation Side Drop – Loading Condition
2.10.3-23 90^0 and 90^0 Orientation Side Drop – Loading Condition
2.10.3-24 45^0 Orientation Side Drop – Basket, P_m (75.5g)
2.10.3-25 45^0 Orientation Side Drop – Basket, $P_m + P_b$ (75.5g)
2.10.3-26 45^0 Orientation Side Drop – Rails, P_m (75.5g)
2.10.3-27 45^0 Orientation Side Drop – Rails, $P_m + P_b$ (75.5g)
2.10.3-28 60^0 Orientation Side Drop – Basket, P_m (75.5g)
2.10.3-29 60^0 Orientation Side Drop – Basket, $P_m + P_b$ (75.5g)
2.10.3-30 60^0 Orientation Side Drop – Rails, P_m (75.5g)
2.10.3-31 60^0 Orientation Side Drop – Rails, $P_m + P_b$ (75.5g)
2.10.3-32 90^0 Orientation Side Drop – Basket, P_m (75.5g)
2.10.3-33 90^0 Orientation Side Drop – Basket, $P_m + P_b$ (75.5g)
2.10.3-34 90^0 Orientation Side Drop – Rails, P_m (75.5g)
2.10.3-35 90^0 Orientation Side Drop – Rails, $P_m + P_b$ (75.5g)
2.10.3-36 180^0 Orientation Side Drop – Basket, P_m (75.5g)
2.10.3-37 180^0 Orientation Side Drop – Basket, $P_m + P_b$ (75.5g)
2.10.3-38 180^0 Orientation Side Drop – Rails, P_m (75.5g)
2.10.3-39 180^0 Orientation Side Drop – Rails, $P_m + P_b$ (75.5g)
2.10.3-40 Hold Down Ring Alignment Leg Finite Element Model with Boundary Conditions

2.10.3-41 Hold Down Ring Finite Element Model with 90° Drop Orientation Boundary Conditions
2.10.3-42 Hold Down Ring Finite Element Model with 45° Drop Orientation Boundary Conditions
2.10.3-43 Small Basket Finite Element Model Locations
2.10.3-44 Small Basket Finite Element Model with Boundary Conditions
2.10.3-45 NUHOMS 61B Basket Model Geometry
2.10.3-46 Vertical Drop Buckling Analysis, Location 1
2.10.3-47 30^0 Drop Buckling Analysis, Location 1
2.10.3-48 45^0 Drop Buckling Analysis, Location 1
2.10.3-49 Vertical Drop Buckling Analysis, Location 2
2.10.3-50 30^0 Drop Buckling Analysis, Location 2
2.10.3-51 45^0 Drop Buckling Analysis, Location 2
2.10.3-52 Allowable Collapse Load Determination, Location 1, Vertical Drop
2.10.3-53 Allowable Collapse Load Determination, Location 1, 30° Drop
2.10.3-54 Allowable Collapse Load Determination, Location 1, 45° Drop
2.10.3-55 Allowable Collapse Load Determination, Location 2, Vertical Drop
2.10.3-56 Allowable Collapse Load Determination, Location 2, 30° Drop
2.10.3-57 Allowable Collapse Load Determination, Location 2, 45° Drop
2.10.3-58 Support Rail Type 1 Location
2.10.3-59 Support Rail Type 1 Finite Element Model with Boundary Conditions
2.10.3-60 NUHOMS 61B Basket Rail Buckling Analysis, Case 1
2.10.3-61 NUHOMS 61B Basket Rail Buckling Analysis, Case 2
2.10.3-62 Support Rail Type 1 Allowable Collapse Load Determination
2.10.3-63 NUHOMS-61B Canister 2-Dimensional Finite Element Model
2.10.3-64 NUHOMS-61B Canister 2-Dimensional Finite Element Model, Including Nodal Couplings and Front End Drop Boundary Conditions, Front Closure
2.10.3-65 NUHOMS-61B Canister 2-Dimensional Finite Element Model, Including Nodal Couplings and Front End Drop Boundary Conditions, Rear Closure

APPENDIX 2.10.3

NUHOMS®-61BT DSC (CANISTER AND BASKET) STRUCTURAL EVALUATION

2.10.3.1 Introduction

Each NUHOMS®-61BT DSC consists of a fuel basket and a canister body (shell, canister inner bottom and top cover plates and shield plugs). The confinement vessel for the NUHOMS®-61BT DSC consists of a shell which is a welded, stainless steel cylinder with an integrally-welded, stainless steel bottom closure assembly, and a stainless steel top closure assembly.

The Canister shell thickness is 0.50 inches, and the bottom and top shield plugs are 5.0 and 7.0 inches. The Canister is constructed from SA-240 Type 304 stainless steel and A-36 carbon steel. There are no penetrations through the confinement vessel. The draining and venting systems are covered by the seal welded outer top closure plate and vent port plug. To preclude air in-leakage, the canister cavity is pressurized above atmospheric pressure with helium.

The basket structure consists of assemblies of stainless steel fuel compartments held in place by basket rails and a hold down ring. The four and nine compartment assemblies are held together by welded stainless steel boxes wrapped around the fuel compartments, which also retain the neutron poison plates between the compartments in the assemblies. The borated aluminum or boron carbide/aluminum metal matrix composite plates (neutron poison plates) provide the necessary criticality control and provide the heat conduction paths from the fuel assemblies to the cask cavity wall. This method of construction forms a very strong structure of compartment assemblies which provide for storage of 61 fuel assemblies. The open dimension of each fuel compartment is 6.0 in. × 6.0 in., which provides clearance around the fuel assemblies.

The Fuel Basket and Canister are analyzed independently. The Fuel Basket is analyzed in Section 2.10.3.2, while the Canister is analyzed in Section 2.10.3.3. Three separate finite element models are constructed for the structural evaluation of the basket and canister. A 3-dimensional cross-section finite element model is utilized to evaluate the effect of transverse impact loads on both the basket and canister. A 3-dimensional model of a Fuel Basket section is used to perform a buckling evaluation for the basket during lateral impact loads. A 2-dimensional axisymmetric model of the canister is used to evaluate the effects of axial impact loads as well as internal and external pressures on the canister alone. Analytical calculations are utilized in order to evaluate axial impact loads applied to the basket, and to perform buckling and fatigue evaluations for the canister.

2.10.3.2 Fuel Basket Structural Analysis

2.10.3.2.1 Approach

The Fuel Basket is evaluated for normal and accident condition impact and thermal loads. The basket stress analysis is performed using a finite element method for the side drop and thermal load cases and analytical calculations for the end drop load cases. Buckling analysis of the basket plates when subjected to lateral impact loads is evaluated by collapse load analysis using a finite element model to generate a relationship between displacement and applied load. A summary of the basket load cases is provided in Section 2.10.3.2.2. Stress and buckling analyses are provided in Sections 2.10.3.2.3 and 2.10.3.2.4 respectively.

Material Properties

The mechanical properties of structural materials used in the basket, rail and canister are shown in the Table 2.10.3-1 as a function of temperature. The materials are identified by reference to ASME Code specifications [3]. The yield and ultimate strengths of the structural steel, shown in Table 2.10.3-1, are the minimum values specified in the material specifications. The following table shows the maximum calculated temperatures from Chapter 3 and the selected allowable stress temperatures for the fuel basket components analyzed.

Component	Max. Calculated Temperature, °F	Selected Allowable Stress Temperature, °F
Basket Rail	482	500
Basket	578	600

Design Criteria

For normal conditions, the basis for the basket allowable stress is the ASME Code, Section III, Subsection NG [1]. The primary membrane stress intensity and membrane plus bending stress intensities are limited to S_m (S_m is the code allowable stress intensity) and 1.5 S_m, respectively, at any location in the basket for Level A (Normal Service) load combinations. The average shear stress is limited to 0.6 S_m.

The ASME Code provides a $3S_m$ limit on primary plus secondary stress intensity for Level A conditions. That limit is specified to prevent ratcheting of a structure under cyclic loading and to provide controlled linear strain cycling in the structure so that a valid fatigue analysis can be performed.

For accident conditions, stresses are evaluated as short duration Level D conditions as per ASME B&PV Code, Section III, Appendix F [2]. When evaluating the results from the non-linear elastic-plastic analysis, the general primary membrane stress intensity, P_m, shall not exceed $0.7S_u$ and the maximum stress intensity at any location (P_l or $P_m + P_b$) shall not exceed 0.9 S_u. The average shear stress is limited to 0.42 S_u.

The allowable stresses for both normal and accident conditions are summarized in the following table.

Loading Condition	Stress Category	Stress Criteria* [10]	Basket Plate Allowable Stress At 600° F (ksi.)	Support Rail Allowable Stress At 500° F (ksi.)
Normal Conditions, Elastic Analysis	Membrane Stress, P_m	S_m	16.40	17.50
	Membrane + Bending Stress, $P_m + P_b$	$1.5\ S_m$	24.60	26.25
	Average Shear Stress	$0.6\ S_m$	9.84	10.50
	Primary + Secondary Stress, $P_m + P_b + Q$	$3\ S_m$	49.20	52.50
Accident Conditions, Elastic-Plastic Analysis	Membrane Stress, P_m	$0.7\ S_u$	44.38	44.38
	Membrane + Bending Stress, $P_m + P_b$	$0.9\ S_u$	57.06	57.06
	Average Shear Stress	$0.42\ S_u$	26.63	26.63

2.10.3.2.2 Loading Conditions

The basket normal and accident condition transport loads are summarized in the tables below.

Basket Normal Condition Loads

Loading	Basket Orientation	Service Level	Load	Analysis Method
Thermal Load	Horizontal	A	100° F Ambient	Finite Element Analysis
1 Foot Side Drop	Horizontal	A	30*g* Lateral Load	Finite Element Analysis
1 Foot End Drop	Horizontal	A	30*g* Axial Load	Analytical Hand Calculation

Basket Accident Condition Loads

Loading	Basket Orientation	Service Level	Load	Analysis Method
30 Foot Side Drop	Horizontal	D	75*g* Lateral Load	Finite Element Analysis
30 Foot End Drop	Horizontal	D	75*g* Axial Load	Analytical Hand Calculation

Each normal and accident condition side and end drop load case is combined with the hot environment thermal load case.

2.10.3.2.3 Fuel Basket Stress Analysis

A. Finite Element Model Description

A three-dimensional ANSYS [4] finite element model of the basket, rails and canister is constructed using SHELL 43 elements. The overall finite element model of the basket, rails and canister is shown in Figure 2.10.3-1. The strength of poison plates is conservatively neglected by excluding these plates from the finite element model. However, the weight of the aluminum plates is accounted for by increasing the stainless steel basket plate density. Because of the large number of plates in the basket and large size of the basket, certain modeling approximations are necessary. Because the rails provide continuous support along the entire length of the basket during a side drop, only a 3 inch long slice of the basket, rail and canister is modeled. At the two cut faces of the model, symmetry boundary conditions are applied (UZ = ROTX = ROTY = 0). The fuel compartment tubes, outer 3 × 3 and 2 × 2 wraps, and basket rails are included in the model and are shown individually in Figures 2.10.3-2 to 2.10.3-4.

The connections between the stainless steel fuel compartments (with intermediate aluminum poison plates) and the outer stainless steel wraps, and between the outer wraps and the stainless steel rails, are made with node couplings. The nodes of various plates are coupled together in the out-of-plane direction so that they will bend in unison under surface pressure or other lateral loads, and to simulate "through the thickness" support provided by the poison plates. Node couplings also simulate the bolt connections between the support rails and the outer boxes.

The canister shell is resting on four sliding rails inside the transport cask (0.12" thick continuous pad) at approximately 18° and 52° on either side of canister/basket centerline (see Figure 2.10.3-5). The basket and canister are analyzed for two side drop scenarios. For each drop scenario, the gap elements between the outside of the canister and inside of the transport cask are simulated in the following way.

Impact Away From the Transport Cask Sliding Rails (Figure 2.10.3-5, 45°, 60° and 90°)

The gap elements (CONTACT 52) are used to simulate the interface between the basket support rails and the inner side of the canister as well as between the outer side of the canister and inside of the cask. Each gap element contains two nodes; one on each surface of the structure. The gap nodes specified at the inner side of cask are restrained in the *x*, *y* and *z* directions. The gap size at each gap element is determined by the difference between the basket rails radius and the inside radius of the canister shell, and by the difference between the canister outer radius and the inside radius of the transport cask. Gap sizes for the gap elements, at each radial location, are determined and inputed into the model as real constants using a small ANSYS macro. This macro accepts the drop orientation and model geometry as inputs and then determines the circumferential position of each gap element. The macro then computes the appropriate real constants and applies to it appropriate gap elements. The gap sizes between the rails and the canister; and between the canister and the cask (over 5° interval up to 90° and 10° interval beyond) are shown in Figures 2.10.3-6 and Figure 2.10.3-7. The finite element model of the canister and gaps is shown in Figure 2.10.3-8 and Figure 2.10.3-9.

Impact On Transport Cask Sliding Rails (Figure 2.10.3-5, 180°)

During the drop on the transport cask sliding rails (180° azimuth side drop), the initial gaps between the canister and the cask are modified. The gaps at the sliding rail locations are assumed to be closed. Between the sliding rail locations, the initial gap size is assumed to be 0.12 inches. The remaining initial gaps are suitably modified (0.12 in. to 0.63 in.) using the ANSYS macro.

During each side drop orientation, some fuel boxes and rails may have a tendency to separate or slide. Gap elements are used to model the connections at such locations. Since the basket is symmetric about the drop axis, for the 90°and 180° side drops, only a one-half model is used for these orientations.

Gap Element Nonlinearities

Gap elements (CONTACT 52) are used to model the actual surface clearance between the basket rails and the inside surface of the canister as well as between the outer surface of the canister and the inside surface of the transport cask. The gap elements also introduce nonlinearities into the model, because the reaction force generated by the gap elements depends on their status (open or closed). The typical gap sizes are shown in Figures 2.10.3-6 and 2.10.3-7. Actual gap sizes at each rail nodal location are computed using an ANSYS macro. The gap element spring constant, K_n, is calculated in the following way.

$$K_n = f\,E\,h \quad [4]$$

Where f is a factor usually between 0.01 and 100, E is the material modulus of elasticity (25.8×10^6 psi), and h and is a typical "target length" or typical element size [typical element length ≈ 1.16 in., typical target length = $(1.16\times3.0)^{0.5}$ = 1.86 in.]. Therefore,

$$K_n = 25.8\times10^6 \times 1.860 \times f = 0.48\times10^6 \text{ to } 4{,}800\times10^6 \text{ lb./in.}$$

In view of the large range in spring constant values, various spring constants were evaluated. Since the structure responded well with a spring constant value of 0.5×10^6 lb./in., this value of K_n is used.

LINK8 elements, coincident to the CONTACT52 elements, were inserted into the ANSYS model to increase model stability. To assure that these elements do not transfer substantial load between the surfaces, a very low modulus of elasticity (E =1,000 psi for radial gaps and E = 100 psi for gaps between boxes), a small area (0.1 in^2), and a density of zero were used as material properties for the LINK8 elements.

B. Normal Condition Side Drop Stress Analysis

A nonlinear stress analysis of the basket structure is conducted in order to compute the elastic stresses for the 45°, 60°, 90°, and 180° drop orientations. The nonlinearity of analysis is due to the gaps in the model. The load resulting from the fuel assembly weight was applied as pressure

on the plates. At 90° and 180° drop orientations, the pressure acted only on the horizontal plates while at other drop orientations, it was divided in components to act on horizontal and vertical plates. The inertia load due to basket, rails and DSC dead weight is simulated using the density and appropriate acceleration. The poison plate weight is included by increasing the basket plate density. A maximum load of 30*g* is applied in each analysis. The automatic time stepping program option AUTOTS is activated. This option lets the program decide the actual size of the load-substep for a converged solution. The program stops at the load substep when it fails to result in a converged solution. In all side drop runs, ANSYS gave converged solutions up to the 30*g* applied load.

The maximum nodal stress intensities for each drop orientation in the basket plates and support rails are listed in Table 2.10.3-2. For shell elements, the middle fiber stresses are classified as membrane stresses (P_m) and top & bottom fiber stresses are classified as membrane plus bending stresses ($P_m + P_b$). These maximum stress intensities are also used to combined with the maximum thermal stresses calculated in Section E of this appendix and compared with the code allowable stresses as listed in Table 2.10.3-2. As shown, all stresses are within the defined allowables.

C. Normal Condition End Drop Stress Analysis

During an end drop, the fuel assemblies and fuel compartment are forced against the bottom of the cask. It is important to note that, for any vertical or near vertical loading, the fuel assemblies react directly against the bottom or top end of the cask and not through the basket structure as in lateral loading. It is the dead weight of basket only that causes axial compressive stress during an end drop. Axial compressive stresses are conservatively computed assuming that all of the basket weight will be taken by the fuel compartments and outer wrappers only. A conservative basket weight of 23,000 lb. (actual weight is 22,918 lb. Section 2.2) is used in end drop stress calculations.

Compressive Stress in the Fuel Compartment Tubes and Outer Wrappers

Total Weight = 23,000 lb.
Weight excluding hold down ring, SS inserts, aluminum plates, and rails is 12,406 lb.
Section area = $12{,}406/(164 \times 0.29) = 260.8$ in^2
Stress due to 1*g* = -23.0 / 260.8 = - 0.09 ksi.
30*g* compressive stress = $-.09 \times 30 = -2.70$ ksi.

Shear Stress in Plate Insert Weld

64 Inserts support the poison plate weight (3,260 lb.).
Load/insert = 3.26 / 64 = 0.051 kips
Weld Shear Area = $0.707 \times 4 \times 0.125 = 0.3535$ in^2
Shear stress (1g) = 0.051 / 0.3535 = 0.15 ksi
At 30g = 0.15 ksi × 30 = 4.50 ksi

Shear Stress in Rail Stud

During 30*g* end drop, the rail will support its own weight. However, the analysis conservatively assumes that the weight of the rail will be supported by the 224 rail studs attached to the outer wrappers.

Weight of rails = 5,350 lb.
Weld Shear Area = $\pi/4\ (0.5^2 - 0.3^2) = 0.126$ in^2
Shear stress (1*g*) = 5.35 / (0.126 × 224) = 0.19 ksi
30*g*, shear stress = 0.19 × 30 = 5.70 ksi

Compressive stress due to end drop on hold down ring

Weight of hold down ring = 940 lb.
Section area = $940/(14.5 \times 0.29) = 223.5$ in^2
Stress due to 1*g* = -23.0/ 223.5= - 0.1 ksi.
30 *g*, compressive stress = -0.1 × 30 = -3.0 ksi.

D. Thermal Expansion Analysis

In this section, the thermal expansions of various components of the NUHOMS-61B basket are evaluated. The thermal load considered is the 100° F ambient normal condition temperature distribution computed in Chapter 3. The mechanical properties of the materials, used in the basket, rail, and canister, are shown in the Table 2.10.3-1 as a function of temperature.

The normal condition thermal analysis of the basket is described in Chapter 3. The thermal analysis is performed to determine the basket temperatures for the condition with maximum solar heating, maximum decay heat from the canister contents, and 100° F daily average ambient air temperature. The temperatures at basket center, top and bottom are reproduced in Figures 2.10.3-10, 2.10.3-11 and 2.10.3-12. The results of the thermal analysis are used to evaluate the effects of axial and radial thermal expansion in the basket components. The following table summarizes the 100° F ambient thermal analysis results from Chapter 3. These results support the selection of basket component temperatures for the subsequent thermal expansion analysis.

Summary of 100° F Ambient Normal Condition Thermal Analysis

Component	Max. Calculated Temperature (°F)	Selected Temperature for Thermal Expansion Analysis (°F)
Canister Shell	388	375**
Basket Plate	578	600
Fuel Cladding	598	600
Cask Body	302	300

** Conservatively using lower temperature for thermal expansion analysis. However, for thermal expansion between canister and cask, the canister temperature is assumed as 400°F.

To verify that adequate clearance exists between the basket and canister cavity for free thermal expansion, the thermal expansions between various components are calculated.

Thermal Expansion between the Length of Fuel Assembly and Canister Cavity

The spent fuel assemblies are assumed to be at 600° F and canister shell temperature at 375° F. The length of the spent fuel assembly when exposed to the hot environment is,

$$L_F = L_T + (L_Z \times \alpha_Z + L_S \times \alpha_S)\,\Delta T.$$

Where for the design basis GE 7×7 (longest BWR fuel):

L_F = Hot length of BWR fuel assembly, in.
L_T = Total length of fuel assembly at room temperature = 176.16 in.
L_Z = Length of Zircaloy guide tube ≅160.47 in.
α_Z = Zircaloy coefficient of thermal expansion = 2.73×10^{-6} in./in.°F at 600° F
L_S = Length of stainless steel per fuel assembly ≅15.69 in.
α_S = Stainless steel coefficient of thermal expansion = 9.8×10^{-6} in./in.°F at 600° F
ΔT = 600° F - 70° F = 530° F

Therefore,

$$L_F = 176.16 + (160.47\times2.73 + 15.69\times9.8)\times10^{-6}\times530 = 176.47 \text{ in.}$$

Allowing 1.25 inchs for irradiation growth of the spent fuel assembly, the total assembly length including thermal expansion is 177.72 inches. The length of the canister cavity at room temperature is 179.38 inches. The minimum length of the canister cavity at 375° F is,

$$L_{CH} = L_{CC} + L_{CC}\times\alpha_C\times\Delta T.$$

Where:

L_{CH} = Hot length of canister cavity, in.
L_{CC} = Minimum canister cavity length at room temperature = 179.38 in.
α_C = Stainless steel coefficient of thermal expansion = 9.42×10^{-6} in./in.°F at 375° F
ΔT = 375°F - 70°F = 305° F

Therefore,

$$L_{CH} = 179.38 + 179.38\times9.42\times10^{-6}\times305 = 179.90 \text{ in.} > 177.72 \text{ in.}$$

Adequate clearance has been provided between the BWR spent fuel assemblies and the canister cavity length to permit free thermal expansion.

Thermal Expansion between the Outer Diameter of the Basket and Inner Diameter of the Canister Cavity

The basket temperature is assumed to be at 600° F and canister shell temperature at 375° F. The maximum outside diameter of the basket when exposed to the hot environment is,

$$D_{BH} = D_{BC} + (D_{BC} \times \alpha_S)\,\Delta T$$

Where:

D_{BH} = Hot outside diameter of basket, in.
D_{BC} = Maximum outside diameter of basket at room temperature = 66.00 in.
α_S = Stainless steel coefficient of thermal expansion = 9.8×10^{-6} in./in. °F at 600° F
ΔT = 600° F -70° F = 530° F

Therefore,

$$D_{BH} = 66.00 + 66.00 \times 9.8\times10^{-6} \times 530 = 66.34 \text{ in.}$$

The minimum inside diameter of the canister cavity at room temperature is 66.25 inches. The minimum inside diameter of the canister cavity at 375° F is,

$$D_{CH} = D_{CC} + (D_{CC} \times \alpha_c)\,\Delta T$$

Where,

D_{CH} = Minimum inside diameter of canister when hot, in.
D_{CC} = Minimum inside diameter of canister cavity at room temperature = 66.25 in.
α_C = Stainless steel coefficient of thermal expansion = 9.42×10^{-6} in./in.°F at 375° F
ΔT = 375° F -70° F = 305° F

Therefore:

$$D_{CH} = 66.25 + 66.25 \times 9.42\times10^{-6} \times 305 = 66.44 \text{ in.} > 66.34 \text{ in.}$$

Adequate clearance has been provided between the outside diameter of the basket and the inside diameter of the canister cavity to permit free thermal expansion.

Thermal Expansion between the Length of Basket (including Basket hold-down Ring) and Canister Cavity

The basket temperature is assumed to be at 600°F and canister shell temperature at 375°F. The length of the basket when hot is,

$$L_{BH} = L_{BC} + (L_{BC} \times \alpha_S)\, \Delta T$$

Where,

L_{BH} = Hot length of basket including basket hold-down ring, in.
L_{BC} = Total length of basket including hold-down ring at room temperature = 178.50 in.
α_S = Stainless steel coefficient of thermal expansion = 9.8×10^{-6} in./in. °F at 600° F
ΔT = 600 °F –70 °F = 530 °F

Therefore,

$$L_{BH} = 178.5 + 178.5 \times 9.8 \times 10^{-6} \times 530 = 179.43 \text{ in.} < 179.90 \text{ in.}$$

Adequate clearance has been provided between the basket and the canister cavity length to permit free thermal expansion.

Thermal Expansion between the Outer Diameter of Canister and Inner Diameter of Cask body

The canister temperature is assumed to be at 400° F and cask body temperature at 300° F. The maximum outside diameter of the canister when exposed to the hot environment is,

$$D_{BH} = D_{BC} + (D_{BC} \times \alpha_S)\, \Delta T$$

Where:

D_{BH} = Hot outside diameter of canister, in.
D_{BC} = Maximum outside diameter of canister at room temperature = 67.35 in.
α_S = Stainless steel coefficient of thermal expansion = 9.5×10^{-6} in./in.°F at 400° F
ΔT = 400° F - 70° F = 330° F

Therefore,

$$D_{BH} = 67.35 + 67.35 \times 9.5 \times 10^{-6} \times 330 = 67.56 \text{ in.}$$

The minimum inside diameter of the cask cavity at room temperature is 68.00 inches. The minimum inside diameter of the cask cavity at 300° F is,

$$D_{CH} = D_{CC} + (D_{CC} \times \alpha_c)\, \Delta T$$

Where:

D_{CH} = Minimum inside diameter of cask cavity when hot, in.
D_{CC} = Minimum inside diameter of cask cavity at room temperature = 68.00 in.
α_C = Stainless steel coefficient of thermal expansion = 9.2×10^{-6} in./in. °F at 300° F
ΔT = 300 °F –70 °F = 230 °F

Therefore,

$$D_{CH} = 68.00 + 68.00 \times 9.2\times10^{-6} \times 230 = 68.14 \text{ in.} > 67.56 \text{ in.}$$

Adequate clearance has been provided between the outside diameter of the canister and the inside diameter of the cask cavity to permit free thermal expansion.

Thermal Expansion between the Length of Canister and Cask Cavity

The canister temperature is assumed to be at 400° F and cask body temperature at 300° F. The length of the canister when exposed to the hot environment is,

$$L_{BH} = L_{BC} + (L_{BC} \times \alpha_S)\, \Delta T$$

Where:

L_{BH} = Hot length of canister, in.
L_{BC} = Maximum length of canister at room temperature = 196.04 in.
α_S = Stainless steel coefficient of thermal expansion = 9.5×10^{-6} in./in.°F at 400° F
ΔT = 400° F - 70° F = 330° F

Therefore,

$$L_{BH} = 196.04 + 196.04 \times 9.5\times10^{-6} \times 330 = 196.65 \text{ in.}$$

The length of the cask cavity at room temperature is 196.88 inches. The minimum length of the canister cavity at 300 °F is,

$$L_{CH} = L_{CC} + L_{CC} \times \alpha_C \times \Delta T$$

Where:

L_{CH} = Hot length of cask cavity, in.
L_{CC} = Minimum cask cavity length at room temperature = 196.88 in.
α_C = Stainless steel coefficient of thermal expansion = 9.2×10^{-6} in./in.°F at 300° F
ΔT = 300° F –70° F = 230° F

Therefore,

$$L_{CH} = 196.88 + 196.88 \times 9.2 \times 10^{-6} \times 230 = 197.30 \text{ in.} > 196.65 \text{ in.}$$

Adequate clearance has been provided between the canister and the cask cavity length to permit free thermal expansion.

Summary of Thermal Expansion Analysis

Based on the results of the above analyses, there is adequate clearance between the various components of the basket, fuel assemblies, canister and cask to allow free thermal expansion. Consequently, no significant stress will develop in the NUHOMS®-61B Fuel Basket due to thermal expansion. The following table summarizes the thermal expansion calculation results from the above analyses.

Thermal Expansion of 61BT Components

Fuel Assembly/Canister Cavity Axial Thermal Expansion					
F.A. Length at 70°F (in.)	Max. F.A. Temp (°F)	F.A. Length Hot	Canister Cavity Length at 70°F (in)	Min. Canister Cavity Temp (°F)	Canister Cavity Length Hot (in)
176.16	600	177.72	179.38	375	179.90
Basket/Canister Diametrical Thermal Expansion					
Basket O.D. at 70°F (in.)	Basket Temp (°F)	Basket O.D. Hot (in)	Canister Cavity I.D. at 70°F (in)	Min. Canister Cavity Temp (°F)	Canister Cavity I.D. Hot (in)
66.0	600	66.34	66.25	375	66.44
Basket(Including Hold Down Ring)/Canister Cavity Axial Thermal Expansion					
Basket Length at 70°F (in.)	Basket Temp (°F)	Basket Length Hot (in)	Canister Cavity Length at 70°F (in)	Min. Canister Cavity Temp (°F)	Canister Cavity Length Hot (in)
178.50	600	179.43	179.38	375	179.90
Canister/Cask Diametrical Thermal Expansion					
Canister O.D. at 70°F (in.)	Canister Temp (°F)	Canister O.D. Hot (in)	Cask Cavity I.D. at 70°F (in)	Min. Cask Cavity Temp (°F)	Cask Cavity I.D. Hot (in)
67.35	400	67.56	68.00	300	68.14
Canister/Cask Axial Thermal Expansion					
Canister Length at 70°F (in.)	Canister Temp (°F)	Canister Length Hot (in)	Cask Cavity Length at 70°F (in)	Min. Cask Cavity Temp (°F)	Cask Cavity Length Hot (in)
196.04	400	196.65	196.88	300	197.30

E. Thermal Stress Analysis

In this section, the thermal stresses due to thermal gradients of various components of the NUHOMS-61B basket are evaluated. The thermal load considered is the 100° F ambient normal condition temperature distribution computed in Chapter 3. The mechanical properties of the materials, used in the basket, rail, and canister, are shown in the Table 1 as a function of temperature.

Thermal stresses in the basket can only be developed if free thermal expansion of the basket is constrained by the peripheral rails or canister. The thermal expansion calculations provided in Section 2.10.3.2.3.D, show that the basket rails are free to grow during maximum operating temperature in the canister. The rails are attached to the basket with bolts in slotted holes. Therefore, the rails also permit free thermal growth of basket boxes. However, the welded spacers at the top and bottom of the basket connect the fuel compartments and outer wrappers to each other. Thermal stresses are calculated at these locations due to radial temperature gradients. Furthermore, thermal stresses are also investigated in the outer wrapper due to thermal growth of the fuel compartments and poison plates and due to axial thermal gradients.

Thermal Stresses in Basket due to Radial Thermal Gradient

Since the basket inserts are located at the top and bottom of the basket, only these sections are analyzed. Figures 2.10.3-11 and 2.10.3-12 show that the radial thermal gradient at the top of the basket is higher than at the bottom of the basket. Also, the maximum temperature at the top of the basket is higher than at the bottom of the basket. Therefore, the top basket section is selected for thermal stress analysis.

A three-dimensional ANSYS [4] finite element model of the basket is used for the thermal stress analyses of the basket. The model used to conduct the side drop structural analysis of the basket is also used for the thermal stress analysis. This finite element model is described in Section 2.10.3.2.3.A. Due to the symmetry of the temperature distribution, only ¼ model of the model is used (see Figure 2.10.3-13). The rails and canister shell are removed since they have no effect on the basket stresses. The CONTACT52 and LINK8 elements are also removed from the model.

An elastic stress analysis of the basket structure is conducted for computing the thermal stresses. The finite element model, along with displacement boundary conditions and couplings, is shown in Figure 2.10.3-14. The nodal temperature distribution from the thermal analysis is applied to obtain the thermal stress model. The resulting shell middle surface nodal stress intensities are the membrane stress intensities, and the top or bottom surface stress intensities are the membrane plus bending stress intensities. The maximum membrane plus bending stress intensity, due the thermal gradient, is 8,799 psi.

Stresses in Outer Wrap due to Thermal Expansion of Inner Boxes and Aluminum Plates

Stresses in the 3-compartment outer wrap will be higher since the 3-compartment contains two aluminum poison plates (see Figure 2.10.3-15). Tensile stress in outer wrap is generated by the differential thermal growth of outer wrapper and aluminum poison plates. The maximum basket plate temperature in the basket plates is 600° F.

The difference in thermal growth, δL, between the outer stainless steel wrap and the aluminum poison plates is,

$$2\times0.31\times(600 - 70)[\alpha_a - \alpha_s] = 2\times0.31\times(600 - 70)[14.2\times10^{-6} - 9.8\times10^{-6}] = 1719\times10^{-6} \text{ in.}$$

Where α_a and α_s are the coefficients of thermal expansion of aluminum and SA-240 Type 304 stainless steel respectively. The inside length of the outer wrap, L, is 19.43 inches ($6 \times 3 + 6 \times 0.135 + 2 \times 0.31$). Conservatively assuming that outer wrap elongates by δL, the tensile stress in the outer wrap is 2,238 psi. ($1719 \times 10^{-6} \times 25.3 \times 10^{6} / 19.43$).

Stresses in Outer Wrap due to Axial Thermal Gradient

The maximum temperature at the axial center of the basket is roughly 600° F (see Figure 2.10.3-10), while the minimum temperature at the bottom of the basket is roughly 450° F (see Figure 2.10.3-12). The coefficient of thermal expansion and modulus of elasticity of SA-240 Type 304 stainless steel at 450° F, α_S and E are 9.6×10^{-6} in./in.°F, 26.2×10^{6} psi. respectively. The width of the 3-compartment wrap is 19.64 inches. The radial thermal growth, δL, of the outer wrap is,

$$\delta L = L\,\Delta T\,\alpha_s$$

At the axial center of the basket, the thermal growth, δL_1, is 0.10201 in. [$19.64 \times (600\ 0 - 70) \times 9.8 \times 10^{-6}$], while at the bottom of the basket, the thermal growth, δL_2, is 0.07165 in. [$19.64 \times (450 - 70) \times 9.6\times10^{-6}$].

Therefore, the difference in thermal growth between the bottom and center of the outer wrap is 0.10201 in. – 0.07165 in. = 0.01518 in.

In order to calculate the stresses due to the axial thermal gradient, a single side of the outer wrap is analyzed as a plate 19.64 in. × 164 in., fixed on all sides. Equations used in this analysis are taken from Roark [5], Table X, Case 41, and are as follows.

a = 164 in. $\quad b$ = 19.64 in. $\quad a/b$ = 8.35 $\quad \alpha$=0.0284 $\quad \beta$= 0.5

The maximum deflection, y, is given by,

$$y = \alpha w b^4 / (Et^3)$$

$$\Rightarrow w = yEt^3 / \alpha b^4$$

At the center of long edge of the plate, the maximum stress, s, is,

$$s = \beta w b^2 / t^2 = (\beta/\alpha) \times [yEt/b^2]$$

$$= (0.5/0.0284) \times [0.01518 \times 26.2\times10^6 \times 0.105/19.64^2] = 1{,}907 \text{ psi}$$

The combined stress at the center of the wrap is therefore, 2238 psi. + 1907 psi. = 4,145 psi.

Summary of the Basket Thermal Stress Analysis

The following table summarizes and combines the thermal stresses calculated above. The combination is conservative, since the maximum stresses due to each individual case at different basket locations are added, irrespective of their locations. This thermal stress is combined with stresses, from side drop and end drop load cases, and compared with the code allowable stresses for normal conditions in Table 2.10.3-2 and for accident conditions in Table 2.10.3-3.

Thermal Stresses in Basket Compartment

Stress due to radial thermal gradient (ksi) (Top)	Stress due to poison plate thickness growth (ksi) (Center)	Stress due to poison plate length growth (ksi) (Center)	Stress due to axial thermal gradient (ksi) (Center)	Combined Stress (ksi)
8.80	2.24	0	1.91	12.95

Basket Rail Thermal Stress Analysis

This section evaluates the thermal stresses in NUHOMS-61B basket rails, generated by temperature distributions resulting from the 100° F. normal condition ambient environment. Thermal stresses can develop in the rails if free thermal expansion of the rails is constrained by the canister. The thermal expansion analysis provided in Section 2.10.3.2.3.D show that the basket rails are free to grow when subjected to the maximum normal condition temperature in the canister. The rails are attached to the basket with bolts in slotted holes, so that the rails permit free thermal growth of the outer wraps. However, thermal stresses occur in the rails due to temperature gradients within the rails themselves. The rail temperatures, taken from the normal condition thermal analysis (Chapter 3), are provided in Figures 2.10.3-16 and 2.10.3-18.

Elastic 3-dimensional ANSYS [4] finite element models of the Type 1 and Type 2 Rails are constructed from the basket model described in Section 2.10.3.2.3.A, and are used to perform the thermal stress analysis. The finite element models of rails, including displacement boundary conditions, are shown in Figures 2.10.3-19 and 2.10.3-20. The mechanical properties of the

materials, used in the basket, rail, and canister, are shown in the Table 2.10.3-1 as a function of temperature.

The following table summarizes the maximum thermal stress intensities in the Rail Type 1 and the Rail Type 2, due to the normal condition temperature distribution. The shell element middle nodal stress intensity is the membrane stress intensity and the element top or bottom nodal stress intensity is the membrane plus bending stress intensity. The maximum thermal stress of 1,758 psi from the Type 2 rail is combined with the side drop and end drop load cases. These combined stresses are compared with the code allowable stresses for normal conditions in Table 2.10.3-2 and for accident conditions in Table 2.10.3-3.

Basket Rail Thermal Stress Analysis Results

Rail Type	Rail Section	Stress Intensity, Top Surface (psi)	Stress Intensity, Bottom Surface (psi)
Type 1	Top ($P_m + P_b$)	1,057	1,084
	Middle (P_m)	808	800
	Bottom ($P_m + P_b$)	716	717
Type 2	Top ($P_m + P_b$)	1,758	1,564
	Middl e (P_m)	1,428	1,228
	Bottom ($P_m + P_b$)	1,227	1,060

F. Summary of Normal Condition Basket Stress Analysis

Table 2.10.3-2 summarizes the normal condition basket stress analysis results and allowable stresses for each individual load, as well as the combination of impact and thermal loads. The allowable for the basket components is taken at 600° F (from Chapter 3, the actual maximum temperature is 578° F). The allowable stress for the support rails is taken at 500° F (from Chapter 3, the actual maximum temperature of the rails is 488° F). All the calculated stresses are less than the ASME Code allowable stresses.

G. Accident Condition Side Drop Stress Analysis and Results

Loading Conditions

The basket is analyzed for two types of side drops using the ANSYS finite element model described in Section 2.10.3.2,3A. First, the canister is assumed to drop away from the transport cask sliding rails. Under this condition, 45°, 60°, and 90° orientation side drops are considered, because they bound all possible orientations. Second, the canister is assumed to drop directly on the transport cask sliding rails at 180° orientation. The lateral load orientation angle is defined in Figure 2.10.3-5. The load resulting from the fuel assembly weight was applied as pressure on the plates. For the 90° and 180° orientations, the pressure was applied only on the horizontal plates, while in other orientations, it was divided into components acting on both the horizontal and vertical plates. The applied 1*g* pressures for all orientations considered are summarized in the following table.

.Fuel Assembly Weight Simulation Based on 1g Load

Drop Orientations	Pressure Applied to Horizontal Plates $P \times \sin\theta$ (psi)	Pressure Applied to Vertical Plates $P \times \cos\theta$ (psi)
45°	0.4887	0.4887
60°	0.5985	0.3456
90° and 180°	0.6911	-

The inertia load due to the basket, rails, and DSC dead weight is simulated by increasing material density and by applying the appropriate acceleration. Increasing the basket plate density accounts for the poison plate weight.

The load distribution for 45, 60, 90 and 180 degree analyses are shown on Figures 2.10.3-21 to 2.10.3-23.

Material Properties

The basket, rails and canister are constructed from SA-240, 304 stainless steel. A bilinear stress-strain relationship is used to simulate the correct nonlinear material behavior for the short term during dynamic loading from the 30 foot side drop impact. The following elastic and inelastic material properties are used in the analysis:

SA-240, 304 Stainless Steel at 500° F [3]	
Modulus of Elasticity, E (psi)	25.8×10^6
Yield Strength (psi)	19,400
Tangent Modulus, E_t (psi)	5% of $E = 1.29 \times 10^6$

The material properties used in the analysis are taken at 500°F. However, the resulting stresses are compared with the allowable stresses at 600°F. This combination is considered conservative, because using higher values of E, S_y and E_t (properties at 500° F) in the analysis results in higher

stresses. Taking material properties at 600° F also yields higher displacements, causing more gaps to close, which reduces stresses further.

Analysis and Results

A nonlinear stress analysis of the fuel basket is conducted to compute the stresses for the 45°, 60°, 90°, and 180° drop orientations. A maximum load of 100g was applied in each analysis. The automatic time stepping program option "Autots" was activated. This option lets the program decide the actual size of the load-substep for a converged solution. Displacements, stresses and forces for each converged substep load were written on ANSYS result files. The program stops at the load substep when it fails to result in a converged solution. In all side drop cases the program gave converged solutions up to 100g load. Results were extracted at the load sub-step nearest to the maximum drop load of 75g. Maximum nodal stress intensities in the basket and rails are shown on Figures 2.10.2-24 to 2.10.2-39 and summarized in Table 2.10.3-3.

H. Accident Condition End Drop Stress Analysis

During an end drop, the fuel assemblies and fuel compartments are forced against the bottom of the cask. It is important to note that, for any vertical or near vertical loading, the fuel assemblies react directly against the bottom or top end of the cask and not through the basket structure as in lateral loading. It is the dead weight of basket only that causes axial compressive stress during an end drop. Axial compressive stresses are conservatively computed assuming that all of the basket weight will be taken by the fuel compartments and outer wraps only. A conservative basket weight of 23,000 lb. (actual weight is 22,918 lb. Section 2.2) is used in end drop stress calculations.

Compressive Stress in the Fuel Compartment Tubes and Outer Wrappers

Total Weight = 23,000 lb.
Weight excluding hold down ring, SS inserts, aluminum plates, and rails is 12,406 lb.
Section area = $12{,}406/(164 \times 0.29) = 260.8$ in^2
Stress due to $1g$ = -23.0 / 260.8 = - 0.09 ksi.
$75g$ compressive stress = $-.09 \times 75 = -6.75$ ksi.

Shear Stress in Plate Insert Weld

52 Inserts support the poison plate weight (3,260 lb.).
Load/insert = 3,260 / 52 = 63 lb.
Weld shear Area = $0.707 \times 4 \times 0.125 = 0.3535$ in^2
Shear stress ($1g$) = 0.063 / 0.3535 = 0.18 ksi
$75g$, shear stress = $0.18 \times 75 = 13.50$ ksi

Shear Stress in Rail Stud

During 30*g* end drop, the rail will support its own weight. However, the analysis conservatively assumes that the weight of the rail will be supported by the 224 rail studs attached to the outer wrappers.

Weight of rails = 5,350 lb.
Weld Shear Area = $\pi/4\ (0.5^2 - 0.3^2) = 0.126\ in^2$
Shear stress (1*g*) = 5.35 / (0.126 × 224) = 0.19 ksi
75*g*, shear stress = 0.19 × 30 = 14.25 ksi

Compressive stress due to end drop on hold down ring

Weight of hold down ring = 940 lb.
Section area = 940/(14.5 × 0.29) = 223.5 in^2
Stress due to 1*g* = -23.0/ 223.5= - 0.1 ksi.
75*g*, compressive stress = -0.1 × 75 = -7.5 ksi.

I. Summary of Accident Condition Basket Stress Analysis

Table 2.10.3-3 summarizes the accident condition basket stress analysis results and allowable stresses for each individual load, as well as the combination of impact and thermal loads. The allowable for the basket components is taken at 600° F (from Chapter 3, the actual maximum temperature is 578° F). The allowable stress for the support rails is taken at 500° F (from Chapter 3, the actual maximum temperature of the rails is 482° F). All the calculated stresses are less than the ASME Code allowables.

J. Basket Hold Down Ring Accident Condition Stress Analysis

In this section, the stresses in the NUHOMS-61B Basket Hold Down Ring and Ring Alignment Leg are evaluated for the accident condition side drop event. The computed stresses are compared the allowable stresses as per ASME B&PV Code, Appendix F [2]. For this evaluation, nominal dimensions are used, and material properties are taken at 500° F.

Alignment Leg Stress Analysis

The hold down ring is captured between the top of the basket and the inside surface of the canister's top shield plug. This prevents axial motion of the hold down ring. The hold down ring is supported in the transverse direction by the canister support ring, and by four alignment legs that mate with holes in the basket support rails.

A simple finite element model is used to calculate stresses in the alignment legs. The three-dimensional ANSYS [1] finite element model is constructed using SHELL43 plastic shell elements. The finite element model along with boundary conditions is shown in Figure 2.10.3-40.

The alignment legs are constructed from SA-240, 304 stainless steel. A bilinear stress-strain relationship is used to simulate the material behavior beyond elastic limit. The following material properties are used [3].

$E = 25.8\times10^6$ psi.
$S_y = 19.4$ ksi.
$S_u = 63.4$ ksi.
Tangent Modulus, $E_T = 5\%$ of $E = 1.29\times10^6$ psi.

The accident condition side drop subjects the basket and hold down ring to 75g lateral load. During a side drop event, the entire inertial load of the hold down ring acts on one alignment leg.

For the purpose of this analysis, the weight of the hold down ring is taken to be 950 lb. (Actual computed weight from Section 2.2, is 940 lb.). Assuming that the hold down ring's inertial load acts equally on the support ring and alignment leg, the load applied to the alignment leg during a side drop event, L, is the following.

$$L = ½ \times (950 \text{ lb.}) \times (75g) = 35{,}625 \text{ lb.}$$

This force is applied to the alignment leg model as a uniformly distributed pressure. This pressure was applied in a number of steps. The automatic time stepping option, AUTOTS, was activated. This option lets the program decide the actual size of the load sub-step for a converged solution. The program stops at the load sub-step that fails to result in a converged solution. A converged solution was obtained for the maximum applied load.

Table 2.10.3-4 summarizes the maximum alignment leg stresses computed by ANSYS. All the calculated stresses are less than the ASME Code allowables.

Alignment Leg Weld Stress Analysis

A 3/8 inch fillet weld connects the alignment leg with the body of the hold down ring.

The methodology for the following analysis is taken from Bednar [6], Table 10.3, Case 4.

$$Z_w = bd + \frac{d^2}{3} = 6\times4 + \frac{4^2}{3} = 29.33 \text{ in}^2.$$

$$Z = 29.33 \times 0.375 = 11.0 \text{ in}^3.$$

The bending moment in the weld, M, is,

$$M = 35{,}625 \times (0.8 + 0.7/2 + 2.0) = 112{,}219 \text{ in.lb.}$$

Therefore, the bending Stress in the alignment leg weld is, $\sigma_b = 112{,}219/11.0 = 10{,}202$ psi., which is less than the allowable stress of 26.63 ksi.

Hold Down Ring Stress Analysis

A two-dimensional finite model is used to calculate stresses in the hold down ring during a 75g side drop event. The ANSYS finite element model is constructed from PLANE42 elements, with the thickness option. The finite element model is shown in Figure 2.10.3-41.

The hold down ring is constructed from SA-240, 304 stainless steel. A bilinear stress-strain relationship is used to simulate the material behavior beyond elastic limit. The following material properties are used [3].

$E = 25.8\times10^6$ psi.
$S_y = 19.4$ ksi.
$S_u = 63.4$ ksi.
Tangent Modulus, $E_T = 5\%$ of E = 1.29×10^6 psi.

The hold down ring is evaluated for 90° and 45° side drop orientations.

90° Orientation Side Drop:

The finite element model and displacement boundary conditions for the 90° orientation are shown in Figure 2.10.3-41. The nonlinear stress analysis was conducted using the ANSYS [4] computer code. A 100g load (y – direction) was applied in a number of steps. The automatic time stepping option, AUTOTS, was activated. This option lets the program decide the actual size of the load sub-step for a converged solution. The program stops at the load sub-step that fails to result in a converged solution. A converged solution was obtained for the maximum applied load.

Table 2.10.3-4 summarizes the maximum hold down ring stresses at the load step corresponding to 75g. The stresses at critical locations were linearized to obtain the membrane (P_m) and membrane plus bending ($P_m + P_b$) stress intensities.

45° Side Drop

The finite element model and displacement boundary conditions for the 45° orientation are shown in Figure 2.10.3-42. The nonlinear stress analysis was conducted using the ANSYS computer code. A 100g load (–70.7g in x-direction and 70.7g in y - direction) was applied in a number of steps. The automatic time stepping option, AUTOTS, was activated. This option lets the program decide the actual size of the load sub-step for a converged solution. The program stops at the load sub-step that fails to result in a converged solution. A converged solution was obtained for the maximum applied load.

Table 2.10.3-3 summarizes the maximum hold down ring stresses at the load step corresponding to 75g. The stresses at critical locations were linearized to obtain the membrane (P_m) and membrane plus bending ($P_m + P_b$) stress intensities.

2.10.3.2.4 Fuel Basket Buckling Analysis

A. Basket Plate Buckling Analysis

Basket assembly stability which includes a buckling evaluation of the wall between fuel compartments at the most highly loaded location for the most challenging drop orientation and a buckling evaluation of the support rails is determined in this section. Fuel compartment stability is demonstrated by performing a buckling evaluation using an ANSYS finite element analysis approach. Additionally, an order of magnitude check on the fuel compartment stability is performed using a hand calculation methodology. An ANSYS finite element analysis approach is used to evaluate support rail buckling.

Fuel Compartment Stability Demonstration Using Finite Element Analysis

Additional analyses are performed in this section to evaluate the outer basket plate stability when the lateral inertial loading is applied at various angles relative to the plates. Analyses are performed for vertical, 30°, and 45° drop angles (Figure 2.10.3-43).

The basic structural element of the basket is considered to be a wall between fuel compartments which consists of one 0.31" thick poison plate (the strength of the poison plates is neglected from the buckling load calculation, but the weight is included) sandwiched between two 0.135" thick stainless steel. The overall dimensions of this outer basket wall are 6.135" high and 6.0" wide. It is assumed that the load due to eight fuel assemblies stacked on 0.135" thick boxes is more severe than the weight of six fuel assemblies on 0.12" thick boxes. The maximum basket plate temperatures at locations 1 and 2 (Figure 2.10.3-43) are 500°F, and 578°F respectively. The buckling analysis of the basket is conservatively performed at temperatures of 550°F for location 1 and 650° F for location 2.

Finite Element Model

A three-dimensional ANSYS finite element model is constructed using a Shell 43 plastic large strain shell element to evaluate the plastic buckling loads for the basket plates at locations 1 and 2 (Figure 2.10.3-43). Shell 43 is well suited to model nonlinear, flat or warped, thin to moderately thick shell structures. The element has six degrees of freedom at each node: translations in the nodal x, y, and z directions and rotations about the nodal x, y, and z axes. The nodes of various plates are coupled together in the out of plane direction so that they will bend in unison under surface pressure loading and to simulate the through thickness support provided by the poison plates. The finite element model simulation is shown in Figure 2.10.3-44.

Geometric Nonlinearities

Since the structure experiences large deformations before buckling, the large displacement option of ANSYS is used. The deflections during each load step are used to continuously redefine the geometry of the structure, thus producing a revised stiffness matrix. If the rate of change in deflection (per iteration) is observed, an estimation of the stability of the structure can

be made. In particular, if the change of displacement at any node is increasing, the loading is above critical and the structure will eventually buckle.

Material Nonlinearities

Material properties for the basket plates, SA-240 Type 304, are taken from ASME Code [3]. The maximum temperatures at locations 1 and 2 are 500° F and 578° F respectively (Chapter 3). However, the material properties at locations 1 and 2 are conservatively taken at 550° F and 650° F respectively. The following table summarizes the material properties at location 1 (550° F), and Location 2 (650° F).

Temperature	550° F (Location 1)	650° F (Location 2)
Modulus of Elasticity, E (psi.)	25.55×10^6	$25.1 \times 10^{6**}$
Yield Strength, S_y (ksi.)	18.9*	18.0***
Ultimate Strength, S_u (ksi.)	63.4	63.4
Tangent Modulus, E_T 5% of E (psi.)	1.2775×10^6	1.255×10^6

* A value of 18.8 ksi. for S_y @ 550° F is conservatively used in the following analysis.
** A value of 25.05×10^6 psi. for E @ 650° F is conservatively used in the following analysis.
*** A value of 17.9 ksi. for S_y @ 650° F is conservatively used in the following analysis.

Applied Loads

The loads applied on the panel model (Figure 2.10.3-43, Locations 1 & 2) were appropriately transferred from full size basket loads. The three critical drop orientations analyzed for basket plates at both locations are the following:

- Vertical (load applied in the direction parallel to the basket plates)
- 30° (load applied at 30° relative to the basket plate direction)
- 45° (load applied at 45° relative to the basket plate direction)

The loads used in vertical, 30, and 45 degree drop analyses are summarized in Table 2.10.3-5. A maximum load of 200g was applied in each analysis. The automatic time stepping program option "Autots" was activated. This option lets the program decide the actual size of the load-substep for a converged solution. The program stops at the load substep when it fails to result in a converged solution. The last load step, with a converged solution, is the plastic instability load for the model. Figure 2.10.3-45 shows the loading conditions.

Boundary Conditions

The ANSYS finite element model conservatively assumes that both ends of column are hinged. However, the stainless steel (0.135" thick) and poison plates forming the panel extend beyond the panel and connect into other panels so that moments can be developed at the top and bottom

panel edges. These reactive end moments will keep the ends from rotating during buckling. "Formulas for Stress and Strain" by Raymond Roark [5], Fourth Edition, Table XV indicates that:

Load Case No. (From Table XV of Roark)	Loading and Edge Condition	Formula for Critical Load (P)
2	End Load Both Ends Hinged	$P = (1)(\pi^2 EI/L^2)$
3	End Load Both Ends Fixed	$P = (4)(\pi^2 EI/L^2)$

Based on the formulas described above, the end conditions selected for the ANSYS model (both ends hinged) are conservative and the calculated allowable compressive load has a large margin of safety.

ANSYS Finite Element Analysis Results

For each orientation, the analysis is solved with successfully higher loading until convergence can no longer be obtained from the FEA model. Stress intensities and displacement patterns, at the last converged substep, are shown on Figures 2.10.3-46 to 2.10.3-51.

As per paragraph F-1340 [2], the acceptability of a component may be demonstrated by collapse load analysis. The allowable collapse load shall not exceed 100% of the plastic analysis collapse load (F-1341.3). The plastic analysis collapse load is defined as that determined by plastic analysis according to the criteria given in II-1430 (F-1321.6(c)) and NB-3213.25.

Using the methodology described in II-1430 (F-1321.6(c)) or NB-3213.25. For each solution step, the maximum displacements are used to determine the collapse load (see Figures 2.10.3-52 through 2.10.3-57). Following table summarizes the allowable buckling loads for each of the drop orientations. The analyses concludes that the maximum allowable buckling load is 96g's, which occurs for the 30° drop case.

Location	Basket Orientation	Last converged Load (g)	Allowable Collapse Load
Location 1 (550° F)	Vertical	112	112
	30°	99	96
	45°	105	100
Location 2 (650° F)	Vertical	187	185
	30°	148	139
	45°	146	140

Alternate Analysis

As an order of magnitude check, the NUHOMS 61B basket plate allowable buckling load and interaction equations as per paragraph NF-3322.1 (e) are evaluated for the 75g side drop. The

most critically loaded panel (Location 1, Figure 2.10.3-43) is evaluated for the vertical and 30° drop orientations, at a temperature of 550°F.

0°drop:

According to ASME Code, Subsection NF, Paragraph NF-3322-1(c)(2)(a) (Level A Condition) [7] and modified as per Appendix F, Paragraph F-1334 (Level D Condition) [2], the compressive stress limit under accident conditions (Level D) when KL/r is less than 120 and $S_u > 1.2\ S_y$ is,

$$F_a = 2S_y\left[0.47 - \frac{KL/r}{444}\right]$$

Where, $K = 0.65$ as recommended by AISC ([8], Table C1.8.1). Since the basket plate is continuously supported, the column is assumed to have fixed ends. The basket plate length is, $L = 6.0$ inches, and the basket plate width, $b = 6.0$ inches. The moment of inertia of the basket plate, I, is,

$$I = b\,h^3/12 = 6 \times (0.58^3 - 0.31^3)\ /\ 12 = 0.0827 \text{ in.}^4$$

Therefore, the area of the plate, $A = 6 \times 2 \times 0.135 = 1.62$ in.^{2}, and the radius of gyration, $r = (I/A)^{1/2} = 0.2259$ in. So,

$$KL/r = 0.65 \times 6.0\ /\ 0.2259 = 17.26$$

Substituting the values given above, the compressive stress limit, F_a, is,

$$F_a = 2 \times 18{,}800\ [0.47 - (17.26)/444] = 16{,}210 \text{ psi}$$

Total weight above bottom panel = 290 lbs.
Therefore, compressive stress at $75g$, $f_a = 290 \times 75\ /1.62 = 13{,}426$ psi

For combined axial compression and bending, equations 20 and 21 of Paragraph NF-3322.1 (e) (1) are:

$$f_a/F_a + C_{mx} f_b\ /\ [1-(f_a\ /F_e)]\ F_b \leq 1 \qquad \text{(Eq.20)}$$

$$f_a\ /(1.4)(0.6)S_y + f_b\ /\ F_b \leq 1 \qquad \text{(Eq.21)}$$

The allowable stresses for the above equations are determined as follows:

	Allowable Stress	ASME Reference
F_b	$1.5\ S_y = 28{,}200$ psi	F-1334.5(c)
C_{mx}	0.6	NF 3322.1(e)(1)(b)
Note	The allowable stress F_a is multiplied by 1.4 as allowed by Paragraph F-1334	

Since there is no column bending during the vertical drop, the interaction equations are reduced to:

Equation 20: $f_a/F_a = 13{,}426/16{,}210 = 0.83 \leq 1$

Equation 21: $f_a/(1.4)(0.6)S_y = 13{,}426/(1.4)(0.6)28{,}200 = 0.57 \leq 1$

<u>30° Drop (load applied at 30° relative to the basket plate direction)</u>

The plate span is treated as a beam-column with fixed ends under axial compression and uniform transverse load ("Formulas for Stress and Strain", Ed. 4, Table VI, Case 10 [5]).
During a 30 degree side drop,

Axial load (75g), $P = 75g \times 290 \cos(30) = 18{,}836$ lb.
Transverse pressure load (75g) = $75g \times 0.8 \sin(30) = 30$ psi.
The distributed transverse load, $w = 30$ psi $\times$ 6.0 in. = 360 lb./in

Moment at beam center,

$$M = wj^2\left[\frac{U/2}{\sin(U/2)} - 1\right]$$

Where,

$$j = \left[\frac{EI}{P}\right]^{1/2} = \left[\frac{(25.55\times10^6)(0.0827)}{118{,}836}\right]^{1/2} = 10.59$$

$$U = \frac{L}{j} = \frac{6.0}{10.59} = 0.567 \text{ rad.} = 32.49°$$

$$M = (360)(10.59^2)\left[\frac{0.569/2}{\sin(32.49/2)} - 1\right] = 542 \text{ in. lb.}$$

Bending stress, $f_b = Mc/I = 542 \times 0.29 / (0.0827) = 1{,}901$ psi.
Axial compressive stress, $f_a = P/A = 18{,}836/1.62 = 11{,}627$ psi.
$C_{mx} = 0.6$ [Appendix F, F-1334.5(c)]
$F_b = 1.5\ S_y = 1.5 \times 18{,}800 = 28{,}200$ psi. (Subsection NF, NF 322.1(e)(1)(b))

The value of F_e is calculated by the formula below per Paragraph F-1334.5(b):

$$F_e = \frac{\pi^2 E}{1.30\left(\frac{kl}{r}\right)^2} = \frac{\pi^2 25.55\times10^6}{1.30(17.26)^2} = 651{,}127\,\text{psi.}$$

Eq.20: $$\frac{f_a}{F_a} + \frac{C_{mx} f_b}{(1 - f_b/F_e)F_b} = \frac{11{,}627}{16{,}210} + \frac{0.6(1{,}901)}{(1 - 1{,}901/651{,}127)28{,}200} = 0.76 \le 1$$

Eq. 21: $$\frac{f_a}{(1.4)(0.6)S_y} + \frac{f_b}{F_b} = \frac{11{,}627}{(1.4)(0.6)18{,}800} + \frac{1{,}901}{28{,}200} = 0.8 \le 1$$

The results of the hand analytical calculations confirm that allowable buckling loads in the basket plates due to a 75G side drop are within acceptable limits.

B. Support Rail Buckling Analysis

There are two types of rails (type 1 & type 2 – see TN Drawing 1093-71-12). The type 2 rail is shorter while the type 1 rail has longer vertical panels. Consequently, the type 1 rail is limiting for buckling. The overall position of this rail and its loading, with respect to the full basket model, are shown in Figure 2.10.3-58.

A nonlinear stress analysis was conducted to evaluate the plastic buckling loads for the rail. The ANSYS computer code was utilized in this analysis. A three-dimensional finite element model of the rail was extracted from the full basket model as described in Section 2.10.3.2.3A. The finite element model of rail and displacement boundary conditions are shown in Figure 2.10.3-59. The rail is constructed from SA-240, Type 304 stainless steel and its material properties at 500° F are as follows:

Material Properties (500°F)

Stainless Steel (SA-240 Type 304)

$E = 25.8 \times 10^6$ psi.
$S_y = 19.4$ ksi.
$S_u = 63.4$ ksi.
Tangent Modulus, $E_T = 5\%$ of E $= 1.29 \times 10^6$ psi.

Applied Loads Calculations

Vertical Load due to weight on top compartments:
(All weights are calculated for a 3 in. basket length)

- Weight of 14 fuel assemblies = 180.55 lb.
- Weight of 8 SS compartment tubes, 0.12" wall = 20.45 lb.
- Weight of 6 SS compartment tubes, 0.135" wall = 17.29 lb.
- Weight of 2×2 outer wrapper, 0.105" wall = 4.71 lb.
- Weight of 3×3 outer wrapper, 0.105" wall = 4.13 lb.
- Weight of poison plates = 17.72 lb.
- Weight of Rail = 8 lbs.

Total weight = 252.85 say 265 lb.
For 200g, total vertical Load = 265×200 = 53,000 lb.
Nonlinear ANSYS runs were made for two different load cases:

In the first case: 53,000 lb. load was applied equally at six nodal locations on the rail (8,833.33 lbs at each node, see Figure 2.10.3-59). Stress intensities and displacement patterns, at the last converged substep (131.5g), are shown in Figure 2.10.3-60.

In the second case: 53,000 lb load was applied using a 2:1 ratio for two middle nodal and four end nodal locations (13,250 lbs at each middle node and 6,625 at each end node, see Figure 2.10.3-59). Stress intensity and displacement patterns, at the last converged substep (160g), are shown in Figure 2.10.3-61. Thus this load case is not bounding.

Using the methodology described earlier for the basket model, the allowable collapse load has been determined for the first load case in Figure 2.10.3-62. The allowable collapse load for the rail is 128g. For other rails and loadings, the allowable collapse load will be higher.

C. Summary of Fuel Basket Buckling Analysis

It is seen from the above basket buckling analyses, that the 30° drop at location 1 is critical, and the minimum allowable collapse load for the basket is 96g.

The results of the Fuel Basket buckling analysis indicate the allowable collapse *g* loads for the NUHOMS®-61B basket are higher than the applied 75g side drop impact load. Therefore basket and rails are structurally adequate with respect to buckling. The following table summarized the collapse loads for the Fuel Basket and rails.

Component	Orientation and Location	Collapse Load
Fuel Basket Plates	30° azimuth drop, at the periphery of the basket near the impact point.	96*g*
Support Rails	0° Azimuth drop, basket rail type 1.	128*g*

2.10.3.3 Canister Structural Analysis

2.10.3.3.1 Approach

A finite element analysis is performed in order to quantify stresses in the NUHOMS-61B Canister generated by transport loads. The applied loads considered are normal and accident condition front end, rear end, and side drops, combined with 50 psig internal and external pressures and 100° F and -20° F environmental conditions. A two-dimensional axisymmetric finite element model is used to evaluate the stresses generated by axisymmetric loads, such as end drop, pressure, and temperature loads. A three-dimensional cross section finite element model is used to evaluate the stresses generated by the asymmetric side drop loads. An elastic analysis is employed for both normal and accident condition axisymmetric load cases, as well as the normal condition side drop (asymmetric) load cases. However, for the accident condition side drop load case, an elastic-plastic analysis is performed.

Material Properties

Since the maximum normal condition canister temperature is 388° F (Chapter 3), the elastic material properties for the canister structural analysis are conservatively taken at 400° F. The elastic analysis canister material properties are as follows.

Canister Shell and Covers (SA-240 Type 304) at 400° F. [3] [9]

$E = 26.5\times10^6$ psi.
$S_u = 64.0$ ksi.
$\nu = 0.3$
$S_y = 20.7$ ksi.
$S_m = 18.7$ ksi.
$\rho = 0.29$

Temperature dependent coefficient of thermal expansion:

Temperature °F	α_T (in./in. °F^{-1})
70	8.5×10^{-6}
100	8.6×10^{-6}
150	8.8×10^{-6}
200	8.9×10^{-6}
250	9.1×10^{-6}
300	9.2×10^{-6}
350	9.3×10^{-6}
400	9.5×10^{-6}

Top and Bottom Shield Plugs (A-36) at 400° F. [3] [9]

$E = 27.7\times10^6$ psi.
$S_u = 58.0$ ksi
$\nu = 0.3$

$S_y = 30.8$ ksi.
$S = 16.6$ ksi.
$\rho = 0.29$

Temperature dependent coefficient of thermal expansion:

Temperature °F	$\alpha_{(T)}$ (in./in. °F^{-1})
70	6.4×10^{-6}
100	6.5×10^{-6}
150	6.6×10^{-6}
200	6.7×10^{-6}
250	6.8×10^{-6}
300	6.9×10^{-6}
350	7.0×10^{-6}
400	7.1×10^{-6}

For the accident condition side drop analysis, the follow elastic-plastic material properties, conservatively taken at 500° F, are the following.

SA-240, 304 Stainless Steel at 500° F [3]	
Modulus of Elasticity, E (psi)	25.8×10^6
Yield Strength (psi)	19,400
Tangent Modulus, E_t (psi)	5% of $E = 1.29 \times 10^6$

Design Criteria

The resulting stresses are compared with the allowable stresses set forth by ASME B&PV Code Subsection NB [10]. The allowable stresses for both normal and accident conditions are summarized in the following table.

Loading Condition	Stress Category	Stress Criteria* [10]	Material	Allowable Stress (ksi.)
Normal Conditions, Elastic Analysis	Membrane Stress, P_m	S_m	SA-240 Type 304	18.7
			A-36	16.6
	Membrane + Bending Stress, $P_m + P_b$	1.5 S_m	SA-240 Type 304	28.1
			A-36	24.9
Accident Conditions, Elastic Analysis	Membrane Stress, P_m	Lesser of 2.4 S_m or 0.7 S_u	SA-240 Type 304	44.8
			A-36	39.8
	Membrane + Bending Stress, $P_m + P_b$	Lesser of 3.6 S_m or S_u	SA-240 Type 304	64.0
			A-36	58.0
Accident Conditions, Elastic-Plastic Analysis	Membrane Stress, P_m	0.7 S_u	SA-240 Type 304	44.8
	Membrane + Bending Stress, $P_m + P_b$	0.9 S_u	SA-240 Type 304	57.6

* S replaces S_m for class 2 materials (A-36)

2.10.3.3.2 Loading Conditions

The load cases considered in this analysis are normal and hypothetical accident condition front and rear end drops. The impact loads are combined with 50 psig internal and external pressure and the 100° F and -20° F ambient environment thermal loads. The following tables summarize both normal and accident condition Canister individual load cases.

Canister Normal Condition Load Cases

Loading	Analysis Type	Service Level	Load	Analysis Method
Hot Environment Thermal Load	Elastic Analysis	A	100° F Ambient	Finite Element Analysis (2D axisymmetric model)
Cold Environment Thermal Load	Elastic Analysis	A	-20° F Ambient	Finite Element Analysis (2D axisymmetric model)
Internal Pressure	Elastic Analysis	A	50 psi. Internal Pressure*	Finite Element Analysis (2D axisymmetric model)
External Pressure	Elastic Analysis	A	50 psi. External Pressure*	Finite Element Analysis (2D axisymmetric model)
1 Foot Side Drop	Elastic Analysis	A	30*g* Lateral Load	Finite Element Analysis (3D cross-section model w/basket)
1 Foot Front End Drop	Elastic Analysis	A	30*g* Axial Load	Finite Element Analysis (2D axisymmetric model)
1 Foot Rear End Drop	Elastic Analysis	A	30*g* Axial Load	Finite Element Analysis (2D axisymmetric model)

* From Chapter 3, the actual canister internal and external pressures, are 9.8 psig. and 5.4 psig. respectively. However, for the canister stress analysis, 50 psig. is conservatively used as the normal condition internal and external pressure. 50 psig. also bounds both canister internal and external accident conditions pressures.

Canister Accident Condition Load Cases

Loading	Analysis Type	Service Level	Load	Analysis Method
30 Foot Side Drop	Elastic-Plastic Analysis	D	75*g* Lateral Load	Finite Element Analysis (3D cross-section model w/basket)
30 Foot Front End Drop	Elastic Analysis	D	75*g* Axial Load	Finite Element Analysis (2D axisymmetric model)
30 Foot Rear End Drop	Elastic Analysis	D	75*g* Axial Load	Finite Element Analysis (2D axisymmetric model)

The individual loads are combined in the following way.

Canister Normal Condition Load Combinations

Load Case	Individual Loads						
	30g Side Drop	30g Front End Drop	30g Rear End Drop	50 psi. Internal Pressure	50 psi. External Pressure	100° F Ambient Environment	-20° F Ambient Environment
1	X			X		X	
2	X				X		X
3		X		X		X	
4		X			X		X
5			X	X		X	
6			X		X		X

Canister Accident Condition Load Combinations

Load Case	Individual Loads						
	75g Side Drop	75g Front End Drop	75g Rear End Drop	50 psi. Internal Pressure	50 psi. External Pressure	100° F Ambient Environment	-20° F Ambient Environment
7	X			X		X	
8	X				X		X
9		X		X		X	
10		X			X		X
11			X	X		X	
12			X		X		X

2.10.3.3.3 2-Dimensional Axisymmetric Finite Element Model

A 2-dimensional axisymmetric finite element model is constructed in order to evaluate the axisymmetric load cases, which include front and rear end drop, internal and external pressure, and temperature loads. A separate 3-dimensional cross-section model, that includes the basket, and is described in Section 2.10.3.2.3.A, is used to evaluate the canister for the side drop load cases.

The 2-dimensional axisymmetric ANSYS [1] finite element model, constructed from PLANE42 elements, is used in this analysis. The elastic material properties listed above are used to model the canister materials. The Canister Lifting Lugs and Grapple are not included in the model. The effect of the unmodeled weight is assumed to be negligible.

The adjacent surfaces of the three front and three rear closure plates are coupled in the axial direction in order to simulate their interaction. Adjacent nodes in the canister shell and closure plates are coupled in both x and y directions at the weld locations.

A plot of the finite element model used in this analysis is shown in Figure 2.10.3-63. An enlarged view front section of the finite element model including nodal couplings and boundary conditions for the front end drop load case is provided in Figure 2.10.3-64. An enlarged view rear section of the finite element model including nodal couplings and boundary conditions for the front end drop load case is provided in Figure 2.10.3-65.

Lid End Drop Boundary Conditions

The weight of the canister internals (basket and fuel assemblies) is accounted for by applying equivalent pressures. The actual weights of the canister basket and fuel assemblies are 22,918 lb. and 43,005 lb. respectively (Section 2.2). Therefore, the total actual weight of the canister internals is 65,923 lb. The weight of the canister internals used in this analysis is conservatively increased to 66,500 lb. The canister cavity inner radius at the front internal edge is 32.375 in. The pressure equivalent to the weight of the internals under normal conditions, P_{in}, is,

$$P_{in} = [\ 66{,}500 / (\pi \times 32.375^2)\ ] \times 30\ gs = 605.862 \text{ psi.}$$

For accident conditions,

$$P_{ia} = [\ 66{,}500 / (\pi \times 32.375^2)\ ] \times 75\ gs = 1514.654 \text{ psi.}$$

Symmetry displacement boundary conditions are applied along the y-axis of the two-dimensional axisymmetric model. The front face of the canister is held in the axial direction in order to simulate the rigid support provided by the transport cask lid. Inertial loads of 30gs and 75gs in the positive y-direction are applied to the model for the normal and accident condition load cases respectively.

Rear End Drop Boundary Conditions

The weight of the canister internals used in this analysis is 66,500 lb. The canister cavity inner radius at the rear internal edge is 33.125 in. The pressure equivalent to the weight of the internals under normal conditions, P_{in}, is,

$$P_{in} = [\ 66{,}500 / (\pi \times 33.125^2)\ ] \times 30\ gs = 578.737 \text{ psi.}$$

For accident conditions,

$$P_{ia} = [\ 66{,}500 / (\pi \times 33.125^2)\ ] \times 75\ gs = 1446.845 \text{ psi.}$$

Symmetry displacement boundary conditions are applied along the y-axis of the 2-dimensionsal axisymmetric model. The rear face of the canister is held in the axial direction in order to simulate the rigid support provided by the transport cask bottom. Inertial loads of 30gs and 75gs in the negative y-direction are also applied to the model for the normal and accident condition load cases respectively.

Thermal Loads

The two temperature distributions applied correspond to the 100° F. and -20° F ambient temperature environments. The temperature distributions used for the 100° F hot environment condition and the -20° F cold environment condition are taken from Chapter 3. Temperatures were applied to the canister modal at several nodes, and a thermal equilibrium analysis was performed, using the material properties provided in Section 2.10.3.3.1, in order to solve for the temperature at the remaining nodes.

2.10.3.3.4 3-Dimensional Cross-Section Finite Element Model

Finite Element Model

A 3-dimensional cross-section finite element model is constructed in order to evaluate the canister for the side drop load cases. This model is also used to evaluate the basket, and is described in detail in Section 2.10.3.2.3.A.

The 3-dimensional finite element model of the basket, rails and canister is constructed using SHELL 43 elements. The overall model is shown in Figure 2.10.3-1. The strength of poison plates is conservatively neglected by excluding these plates from the finite element model. However, the weight of the aluminum plates is accounted for by increasing the stainless steel basket plate density. Because of the large number of plates in the basket and large size of the basket, certain modeling approximations are necessary. Because the rails provide continuous support along the entire length of the basket during a side drop, only a 3 inch long slice of the basket, rail and canister is modeled. At the two cut faces of the model, symmetry boundary conditions are applied (UZ = ROTX = ROTY = 0). The fuel compartment tubes, outer 3 × 3 and 2 × 2 boxes, and rails are included in the model and are shown individually in Figures 2.10.3-2 to

2.10.3-4. The gap elements (CONTACT 52) are used to simulate the interface between the basket rails and the inner side of the canister as well as between the outer side of the canister and inside of the cask are described in detail in Section 2.10.3.2.3.A. The model is used to analyze the canister for both normal and accident conditions.

Loading Conditions

The canister is analyzed for two types of side drops using the ANSYS finite element model described in Section 2.10.3.2.3 A. First, the canister inside the cask is assumed to drop away from the transport cask sliding rails. Under this condition, 45°, 60°, and 90° orientation side drops are assumed to bound all possible orientations. Second, the side drop occurs on the transport cask sliding rails in the 180° orientation. The lateral load orientation angle is defined in Figure 2.10.3-5. The load resulting from the fuel assembly weight was applied as pressure on the plates. In the 90° and 180° orientations, the pressure is applied only on the horizontal plates while in other orientations, it is divided into components that act on both the horizontal and vertical plates. The 1g pressures for the different orientations considered are summarized in the following table.

Fuel Assembly Weight Simulation Based on 1g Load

Drop Orientations	Pressure Applied to Horizontal Plates $P \times \sin\theta$ (psi)	Pressure Applied to Vertical Plates $P \times \cos\theta$ (psi)
45°	0.4887	0.4887
60°	0.5985	0.3456
90° and 180°	0.6911	-

The inertia load due to basket, rails, and canister dead weight is simulated using the density and appropriate acceleration. The poison plate weight is accounted for by increasing the basket plate density.

The load distribution for the 45°, 60°, 90°, and 180° analyses are shown on Figures 2.10.3-21 to 2.10.3-23.

2.10.3.3.5 Stress Analysis Results

The maximum stress intensities in the canister are extracted from the ANSYS results, from both models, for all twelve load combinations. These stresses are compared to the normal and accident condition code allowables. Tables 2.10.3-6 and 2.10.3-7 summarize the maximum calculated and allowable stress intensities generated in the NUHOMS®-61BT Canister for normal and accident conditions respectively.

For the end drop load combinations, both normal and accident condition allowable stresses are taken to be the normal and accident condition membrane allowable stresses for SA-240 Type

304, because the maximum stresses occur in the canister shell region (SA-240, Type 304 material), and stresses in the shield plugs (A-36 material) are small.

For the accident condition side drop load combinations, the maximum calculated elastic stress intensity generated by temperature and pressure loads are conservatively added to the maximum calculated elastic-plastic stress intensity generated by the side drop load cases. The resulting combined stress intensities are conservatively compared to the accident condition plastic analysis stress limits.

2.10.3.3.6 Canister Buckling Analysis

In this section, The analytical method provided in ASME Code Case N-284-1 [11] is used to determine the adequacy of the NUHOMS®-61BT canister with respect to buckling due to axial compression and external pressure.

Since the vessel is assumed to be unstiffened, only the theoretical bhuckling calculation for unstiffened shells or local buckling between stiffeners of stiffened shells applies ([11] Section 1712.1). Code Case N-284-1, Section –1712.2, Stringer Buckling and General instability, does not apply since it analyzes the global buckling of a stinger stiffened vessel.

Applied Loads

The canister normal and accident condition buckling loads are summarized in the tables below.

Canister Normal Condition Buckling Loads

Loading	Service Level	Load
External Pressure	A	15 psi. external pressure*
1 Foot End Drop	A	30*g* Axial Load

* From Chapter 3, the actual normal condition canister external pressure is 5.4 psig. However, for the normal condition buckling analysis, 15 psig. is conservatively used.

Canister Accident Condition Buckling Loads

Loading	Service Level	Load
External Pressure	D	22 psi. external pressure*
30 Foot End Drop	D	75*g* Axial Load

* From Chapter 3, the actual accident condition canister external pressure is 9.4 psig. However, for the accident condition buckling analysis, 22 psig. is conservatively used.

Material Properties

Properties of Canister Shell and Covers (SA-240 Type 304) at 500° F. [3]

$E = 25.8\times10^6$ psi.	$S_y = 19.4$ ksi.
$S_u = 63.4$ ksi.	$S_m = 17.5$ ksi.
$\nu = 0.3$	$\rho = 0.29$

Notation

The following notations are taken from ASME Code Case N-284-1 [11], Section –1200.

- Subscripts ϕ and θ = axial (meridional) and circumferential directions respectively.
- l_ϕ = distances between lines of support in the axial direction, use 179.3 in.
- R = shell radius, mean radius = [66.25 inner diameter + 67.25 outer diameter] / 4 = 33.375 in.
- t = shell thickness, 0.5 in.
- $M_\phi = \dfrac{l_\phi}{\sqrt{(R)(t)}}$
- C_ϕ, C_θ = elastic buckling coefficient under external pressure and axial compression respectively.
- σ_{heL}, $\sigma_{\phi eL}$ = local theoretical elastic instability stress in the hoop direction for cylinders under external pressure and axial compression respectively, psi.
- E = modulus of elasticity of the material at design temperature, 25.8×10^6 psi. @ 500° F, (Ref. 3).
- $\alpha_{\theta L}$ = capacity reduction factor to account for the difference between classical theory and predicted instability stresses for fabricated shells.
- σ_y = tabulated yield stress of material at design temperature, 19,400 psi. @ 500° F (Ref. 3).
- σ_{ha}, σ_{rc}, allowable stresses for elastic and inelastic buckling respectively, psi.
- FS = factor of Safety, 2 for normal conditions, 1.34 for accident conditions (Ref. 1, Section –400 (a)).

Compressive Stress due to End Drop

The canister wall resists the weight of the shell plus the weight of top end components during a bottom end drop event. The total weight of these items is 14,950 lb. (Section 2.2). The corresponding applied force generated for a 1g end drop, F_{axial}, is,

$$F_{axial} = 14{,}950 \text{ lb.} \times 1g = 14{,}950 \text{ lb.}$$

The cross sectional area, A, of the container shell is the following.

$$A = \frac{\pi}{4}\left[D_o^2 - D_i^2\right] = \frac{\pi}{4}\left[67.25^2 - 66.25^2\right] = 104.85 \text{in.}^2$$

Therefore, the compressive stress applied to the canister shell for 1g end drop is,

$$\sigma_a = P / A = 14{,}950 \text{ lb.} / 104.85 \text{ in.}^2 = 142.58 \text{ psi.}$$

For 30g deceleration due to normal condition load, $\sigma_n = 142.58 \times 30g = 4{,}278$ psi.

For 75g deceleration due to accident condition load, $\sigma_a = 142.58 \times 75 = 10{,}694$ psi.

Shell Stress due to External Pressure

The hoop stress, σ_{hoop}, generated by external pressure is governed by the following formula.

$$\sigma_{hoop} = \frac{PR}{t}$$

Where P is the external pressure applied, R is the mean radius of the shell, and t is the shell thickness. For normal condition external pressure of 15 psi., the corresponding hoop stress, σ_{np}, is,

$$\sigma_{np} = \frac{(15)(33.375)}{0.5} = 1{,}001 \text{ psi.}$$

For accident condition external pressure of 22 psi., the corresponding hoop stress, σ_{np}, is,

$$\sigma_{ap} = \frac{(22)(33.375)}{0.5} = 1{,}469 \text{ psi.}$$

Shell Buckling due to Compressive Stress

- Theoretical Buckling Value

Local Buckling ([11] Section –1712.1.1 (a)):

$$M_\phi = \frac{l_\phi}{\sqrt{(R)(t)}} = \frac{179.3}{\sqrt{(33.375)(0.5)}} = 43.89 \text{ in.}$$

$$\Rightarrow M_\phi > 1.73$$

Therefore,

$$C_\theta = 0.605$$

$$\Rightarrow \sigma_{\phi eL} = C_\theta \frac{(E)(t)}{R} = 0.605 \frac{(25.8\times10^6)(0.5)}{33.375} = 0.2338\times10^6 \text{ psi.}$$

- Capacity Reduction Factor

From Code Case N-284-1, Section –1511 (a), for local buckling of cylindrical shells, stiffened or unstiffened under Axial Compression, $\alpha_{\phi L}$ is the larger of (1) and (2).

(1) Effect of *R/t*

$$\frac{R}{t} = \frac{33.375}{0.5} = 66.75$$

$$\Rightarrow \alpha_{\phi L} = MIN\left\{\begin{array}{c} 1.52 - 0.473\log_{10}\left(\frac{R}{t}\right) = 0.657 \\ \frac{300\sigma_y}{E} - 0.033 = 0.193 \end{array}\right\} = 0.193$$

(2) Effect of Length

$$M_\phi = 43.89 > 10 \Rightarrow \alpha_{\phi L} = 0.207$$

Therefore, $\alpha_{\phi L} = 0.207$.

- Plasticity Reduction Factor

The plasticity reduction factor is computed based on the formulae provided in Code Case N-284-1, Section –1611 (b) as follows.

$$\Delta = \frac{\alpha_{\theta L}\sigma_{\phi eL}}{\sigma_y} = \frac{(0.207)(0.2338\times10^6)}{19{,}400} = 2.49$$

Since $1.6 < \Delta <$ Local Buckling ([11], Section –1712.1.1 (b) (2)): 6.25,

$$\eta_\phi = \frac{1.31}{1+1.15\Delta} = \frac{1.31}{1+1.15x2.49} = 0.34 .$$

Shell Buckling due to External Pressure

The analytical method provided in ASME Code Case N-284-1 is used to determine that the NUHOMS-61B Transportable Storage Canister is structurally adequate with respect to buckling due to external pressure with end pressure included.

- Theoretical Buckling Value

$$(\sigma_\phi = 0.5\ \sigma_\theta)$$

$$M_\phi = \frac{l_\phi}{\sqrt{(R)(t)}} = \frac{179.3}{\sqrt{(33.375)(0.5)}} = 43.89 \text{ in.}$$

$$\frac{R}{t} = \frac{33.375}{0.5} = 66.75 \quad \text{and} \quad 1.65\ \frac{R}{t} = 110.14$$

$$\Rightarrow 3.5 < M_\phi < 1.65\ \frac{R}{t}$$

Therefore,

$$C_{\theta h} = \frac{0.92}{M\phi - 0.636} = \frac{0.92}{43.89 - 0.636} = 0.0213$$

$$\Rightarrow \sigma_{heL} = C_{\theta h}\frac{(E)(t)}{R} = 0.0213\frac{(25.8\times10^6)(0.5)}{33.375} = 8{,}233 \text{ psi.}$$

- Capacity Reduction Factor

From Code Case N-284-1, Section –1511 (b), for local buckling of cylindrical shells, stiffened or unstiffened under Hoop Compression,

$$\alpha_{\theta L} = 0.8$$

- Plasticity Reduction Factor

The plasticity reduction factor is computed based on the formulae provided in Code Case N-284-1, Section –1611 (b) as follows.

$$\Delta = \frac{\alpha_{\theta L}\sigma_{heL}}{\sigma_y} = \frac{(0.8)(8{,}233)}{19{,}400} = 0.340$$

Since $\Delta < 0.67$,

$$\eta_\theta = 1$$

Summary of Buckling Results

The calculated buckling results for the end drop and external pressure are summarized in the following table.

Item	End Drop (axial direction)		External Pressure (hoop direction)	
	Normal (30g)	Accident (75g)	Normal (15 psi)	Accident (22 psi)
Calculated Stress (psi)	4,278	10,694	1,001	1,469
Factor of Safety	2.0	1.34	2.0	1.34
F.O.S Amplified Stress (psi)	8,556	14,330	2,002	1,969
Capacity Reduction Factor	0.207	0.207	0.8	0.8
Elastic Amplified Stress (psi)	41,333	69,227	2,503	2,461
Plastic Reduction Factor	0.34	0.34	1.0	1.0
Plastic Amplified Stress (psi)	121,568	203,609	2,503	2,461
Theoretical Buckling Stress (psi)	233,800	233,800	8,233	8,233

Interaction Equations for Local Buckling ([11], Section – 1713)

- Normal Condition

The combination of axial compression from the 30*g* end drop with 15 psi normal condition external pressure is analyzed using the interaction equation provided in Code Case N-284, Section –1713.

The combined axial membrane stress is, $\sigma_\phi = 4{,}278 + 1{,}001/2 = 4{,}779$ psi, and the hoop membrane stress is, $\sigma_\theta = 1{,}001$ psi. Therefore,

$$\sigma_{xa} = \frac{(\alpha_{\phi L})(\sigma_{\phi eL})}{FS} = \frac{(0.207)(0.2338\times10^6)}{2.0} = 24{,}198 \text{ psi.}$$

$$t_\theta = t_\phi = t$$
$$t_\theta / t_\phi = 1.0$$

Since, $K > 0.5$ and $\sigma_\phi \geq 0.5\sigma_{ha}$, the interaction equations in Section –1713.1.1 (b) apply.

$$\frac{\sigma_\phi - 0.5\sigma_{ha}}{\sigma_{xa} - 0.5\sigma_{ha}} + \left(\frac{\sigma\theta}{\sigma_{ha}}\right)^2 \leq 1.0$$

$$\frac{4{,}779 - 0.5\times3{,}293}{24{,}198 - 0.5\times3{,}293} + \left(\frac{1{,}001}{3{,}293}\right)^2 = 0.231$$

Therefore, the interaction equation is satisfied.

- Accident Condition

The axial compression generated during the accident condition end drop is combined with the normal condition external pressure load using the interaction equation provided in Code Case N-284-1, Section –1713. Since the accident condition pressure load is generated during the thermal accident, which occurs subsequent to the 30 foot accident condition free drop, it need not be combined with any other load case. However, the axial compression from the 75*g* end drop is conservatively combined with an external pressure of 22 psi.

The combined axial membrane stress is, σ_ϕ = 10,694 + 1,469/2 = 11,429 psi., and the hoop membrane stress is, σ_θ = 1,469 psi. Therefore,

$$\sigma_{xa} = \frac{(\alpha_{\phi L})(\sigma_{\phi eL})}{FS} = \frac{(0.207)(0.2338\times10^6)}{1.34} = 36{,}117 \text{ psi.}$$

$$t_\theta = t_\phi = \text{t}$$
$$t_\theta / t_\phi = 1.0$$

Since, $K > 0.5$ and $\sigma_\phi \geq 0.5\sigma_{ha}$, the interaction equations in Code Case N-284-1, Section –1713.1.1 (b) apply.

$$\frac{\sigma_\phi - 0.5\sigma_{ha}}{\sigma_{xa} - 0.5\sigma_{ha}} + \left(\frac{\sigma\theta}{\sigma_{ha}}\right)^2 \leq 1.0$$

$$\frac{11{,}429 - 0.5x4915}{36{,}117 - 0.5x4915} + \left(\frac{1{,}469}{4{,}915}\right)^2 = 0.355$$

Therefore, the interaction equation is satisfied.

Summary of Buckling Evaluation

From the analysis presented above, it can be seen that all of the stresses generated in the NUHOMS®-61BT Canister are less than their corresponding allowable buckling stresses, and all buckling interaction equation requirements are also met. Therefore the canister will not buckle when subjected to normal or accident condition loads.

2.10.3.4 References

1. American Society of Mechanical Engineers, ASME Boiler and Pressure Vessel Code, Section III, Subsection NG, 1998 with 1999 Addenda.

2. American Society of Mechanical Engineers, ASME Boiler and Pressure Vessel Code, Section III, Appendix F, 1998 with 1999 Addenda.

3. American Society of Mechanical Engineers, ASME Boiler and Pressure Vessel Code, Section II, Part D, 1998, including 1999 addenda.

4. ANSYS Engineering Analysis System, User's Manual for ANSYS Rev 5.6, Swanson Analysis Systems, Inc., Houston, PA, 1998.

5. Roark, Raymond J., *Formulas for Stress and Strain*, Fourth Edition, McGraw-Hill Book Company.

6. Bednar, Henry H., *Pressure Vessel Design Handbook*, Van Nostrand Reinhold Company, 1981.

7. American Society of Mechanical Engineers, ASME Boiler and Pressure Vessel Code, Section III, Subsection NF, 1998 with 1999 Addenda.

8. *Manual of Steel Construction*, Eighth Edition, American Institute of Steel Construction, Inc., 1980.

9. Baumeister & Marks, *Standard Handbook for Mechanical Engineers*, 7th Edition.

10. American Society of Mechanical Engineers, ASME Boiler and Pressure Vessel Code, Section III, Subsection NB, 1998 with 1999 Addenda.

11. Cases of ASME Boiler and Pressure Vessel Code, Case N-284-1, *Metal Containment Shell Buckling Design Methods*, Section III, Division 1, Class MC, 1998 with 1999 Addenda.

12. NUREG/CR-0497-Rev 2,"MATPRO-Version 11 (Revision 2), A handbook of materials properties for use in the analysis of light water reactor fuel rod behavior.

Table 2.10.3-1
Temperature Dependent Material Properties

Component	Material	Temp. °F	Ultimate S_u (ksi)	Yield S_y (ksi)	Allow. S_m (ksi)	E (10^6 psi)	α (10^{-6})
Basket, Rail and Canister	SA-240 Stainless Steel 304 [3]	70	75.0	30.0	20.0	28.3	8.5
		200	71.0	25.0	20.0	27.6	8.9
		300	66.2	22.4	20.0	27.0	9.2
		400	64.0	20.7	18.7	26.5	9.5
		500	63.4	19.4	17.5	25.8	9.7
		600	63.4	18.4	16.4	25.3	9.8
		650	63.4	18.0	16.2	25.1	9.9
Fuel Tube	Zircalloy [12]	600					2.73

Table 2.10.3-2
Summary of Basket Normal Condition Stress Analysis

Drop Orientation	Component	Stress Category	Max. Stress Due to 1 foot drop (ksi)	Max. Thermal Stress (ksi)	Combined Stress (ksi)	Allowable Stress (ksi)
End Drop	Fuel Compartment & Outer Wrapper	P_m	2.7	-	2.7	16.40
		$P_m + P_b + Q$	2.7	12.95	15.65	49.20
	Plate Insert Weld	Shear	4.50	-	4.50	9.84
	Rail Stud	Shear	5.70	-	5.70	9.84
	Hold Down Ring	P_m	3.0	-	3.00	16.40
45° Side Drop	Basket	P_m	6.42	-	6.42	16.40
		$P_m + P_b$	22.72	-	22.72	24.60
		$P_m + P_b + Q$	29.85	12.95	42.80	49.20
	Rails	P_m	5.81	-	5.81	17.50
		$P_m + P_b$	19.19	-	19.19	26.25
		$P_m + P_b + Q$	22.22	1.76	23.98	52.50
60° Side Drop	Basket	P_m	8.14	-	8.14	16.40
		$P_m + P_b$	21.30	-	21.30	24.60
		$P_m + P_b + Q$	29.25	12.95	42.20	49.20
	Rails	P_m	9.49	-	9.49	17.50
		$P_m + P_b$	25.03	-	25.03	26.25
		$P_m + P_b + Q$	30.88	1.76	32.64	52.50
90° Side Drop	Basket	P_m	7.92	-	7.92	16.40
		$P_m + P_b$	13.75	-	13.75	24.60
		$P_m + P_b + Q$	13.75	12.95	26.70	49.20
	Rails	P_m	15.17	-	15.17	17.50
		$P_m + P_b$	26.11	-	26.11	26.25
		$P_m + P_b + Q$	26.11	1.76	27.87	52.50
180° Side Drop, Impact on support rails	Basket	P_m	6.32	-	6.32	16.40
		$P_m + P_b$	11.98	-	11.98	24.60
		$P_m + P_b + Q$	11.98	12.95	24.93	49.20
	Rails	P_m	13.62	-	13.62	17.50
		$P_m + P_b$	18.24	-	18.24	26.25
		$P_m + P_b + Q$	18.24	1.76	20.00	52.50

Table 2.10.3-3
Summary of Basket Accident Condition Stress Analysis

Drop Orientation	Component	Stress Category	Max. Stress Due to 1 foot drop (ksi)	Max. Thermal Stress (ksi)	Combined Stress (ksi)	Allowable Stress (ksi)
End Drop	Fuel Compartment & Outer Wrapper	P_m	6.75	-	6.75	44.38
		$P_m + P_b + Q$	6.75	12.95	19.70	57.06
	Plate Insert Weld	Shear	11.25	-	11.25	26.63
	Rail Stud	Shear	14.25	-	14.25	26.63
	Hold Down Ring	P_m	7.5	-	7.5	44.38
45° Side Drop	Basket	P_m	14.54	-	14.54	44.38
		$P_m + P_b$	27.12	-	27.12	57.06
		$P_m + P_b + Q$	27.12	12.95	40.07	57.06
	Rails	P_m	16.52	-	16.52	44.38
		$P_m + P_b$	25.27	-	25.27	57.06
		$P_m + P_b + Q$	25.27	1.76	27.03	57.06
60° Side Drop	Basket	P_m	14.43	-	14.43	44.38
		$P_m + P_b$	27.30	-	27.3	57.06
		$P_m + P_b + Q$	27.30	12.95	40.25	57.06
	Rails	P_m	20.85	-	20.85	44.38
		$P_m + P_b$	28.72	-	28.72	57.06
		$P_m + P_b + Q$	28.72	1.76	30.48	57.06
90° Side Drop	Basket	P_m	18.02	-	18.02	44.38
		$P_m + P_b$	22.78	-	22.78	57.06
		$P_m + P_b + Q$	22.78	12.95	35.73	57.06
	Rails	P_m	29.03	-	29.03	44.38
		$P_m + P_b$	32.79	-	32.79	57.06
		$P_m + P_b + Q$	32.79	1.76	34.55	57.06
180° Side Drop, Impact on support rails	Basket	P_m	17.18	-	17.18	44.38
		$P_m + P_b$	22.54	-	22.54	57.06
		$P_m + P_b + Q$	22.54	12.95	35.49	57.06
	Rails	P_m	19.01	-	19.01	44.38
		$P_m + P_b$	28.16	-	28.16	57.06
		$P_m + P_b + Q$	28.16	1.76	29.92	57.06

Table 2.10.3-4
Summary of Hold Down Ring Accident Condition Stress Analysis

Drop Orientation	Component	Stress Category	Max. Stress Due to 1 foot drop (ksi)	Allowable Stress (ksi)
Side Drop (All Orientations)	Alignment Leg	P_m	14.06	44.38
		$P_m + P_b$	36.77	57.06
	Alignment Leg Weld	$P_m + P_b$	10.20	57.06
Side Drop (90° Orientations)	Hold Down Ring Body	P_m	1.52	44.38
		$P_m + P_b$	45.91	57.06
Side Drop (45° Orientations)	Hold Down Ring Body	P_m	1.65	44.38
		$P_m + P_b$	34.71	57.06

Table 2.10.3-5
Summary of Loads Used for Different Drop Orientations

Location 1
($F_y = F\cos\theta$, $P_x = P\sin\theta$, $F = 290$ lbs, $P = 0.8$ psi)

Drop Orientation (Degree)	1G load (6" Length) (Weight including all SS & poison plates above the bottom panel, rails, and 8 fuel assemblies**)		200 G Load Computer Run	
	Axial Load F_y (lbs)	Trans. Load P_x (psi)	F_y (lbs)	P_x(psi)
Vertical	290	0	58,000	0
30	251	0.4	50,200	80
45	205	0.565	41,000	113

** This assumption is very conservative for drop orientations other than the vertical drop. For example, for 30 and 45 degree drops, the bottom panel only supports 6 fuel assemblies but was analyzed for 8 fuel assemblies.

Location 2
($F_y = F\cos\theta$, $P_x = P\sin\theta$, $F = 160$ lbs, $P = 0.8$ psi)

Drop Orientation (Degree)	1G load (6" Length) (Weight including all SS & poison plates above the bottom panel, rails, and 4 fuel assemblies**)		200 G Load Computer Run	
	Axial Load F_y (lbs)	Trans. Load P_x (psi)	F_y (lbs)	P_x (psi)
Vertical	160	0	32,000	0
30	139	0.4	27,800	80
45	113	0.565	22,600	113

** This assumption is also very conservative for drop orientations other than vertical drop. For example, for 30 and 45 degree drops, the bottom panel only supports 3 fuel assemblies but was analyzed for 4 fuel assemblies.

Table 2.10.3-6
Summary of Canister Normal Condition Stress Analysis

Load Combination		Stress Category	Maximum Stress (ksi.)	Allowable Membrane Stress Intensity (ksi.)
30*g* Front End Drop	External Pressure, Cold Environment	$P_m + P_b$	9.2	18.7*
	Internal Pressure, Hot Environment	$P_m + P_b$	9.0	18.7*
30*g* Rear End Drop	External Pressure, Cold Environment	$P_m + P_b$	11.6	18.7*
	Internal Pressure, Hot Environment	$P_m + P_b$	10.3	18.7*
45° Azimuth 30g Side Drop	External Pressure, Cold Environment	P_m	6.2	18.7
		$P_m + P_b$	15.1	28.1
	Internal Pressure, Hot Environment	P_m	11.4	18.7
		$P_m + P_b$	20.4	28.1
60° Azimuth 30g Side Drop	External Pressure, Cold Environment	P_m	6.4	18.7
		$P_m + P_b$	19.3	28.1
	Internal Pressure, Hot Environment	P_m	11.6	18.7
		$P_m + P_b$	24.6	28.1
90° Azimuth 30g Side Drop	External Pressure, Cold Environment	P_m	6.6	18.7
		$P_m + P_b$	12.4	28.1
	Internal Pressure, Hot Environment	P_m	11.8	18.7
		$P_m + P_b$	17.7	28.1
180° Azimuth 30g Side Drop	External Pressure, Cold Environment	P_m	7.2	18.7
		$P_m + P_b$	15.0	28.1
	Internal Pressure, Hot Environment	P_m	12.5	18.7
		$P_m + P_b$	20.2	28.1

*The stress intensities (membrane + bending) generated in the canister during the end drop events are conservatively compared with the membrane allowable stress, P_m for SA-240, Type 304.

Table 2.10.3-7
Summary of Canister Accident Condition Stress Analysis

Load Combination		Stress Category	Maximum Stress (ksi.)	Allowable Membrane Stress Intensity (ksi.)
75*g* Front End Drop	Hot Environment, Internal Pressure	$P_m + P_b$	13.6	44.8*
	Cold Environment, External Pressure	$P_m + P_b$	16.8	44.8*
75*g* Rear End Drop	Hot Environment, Internal Pressure	$P_m + P_b$	17.8	44.8*
	Cold Environment, External Pressure	$P_m + P_b$	17.0	44.8*
45° Azimuth 75*g* Side Drop	External Pressure, Cold Environment	P_m	7.2	44.8
		$P_m + P_b$	24.8	57.6
	Internal Pressure, Hot Environment	P_m	12.4	44.8
		$P_m + P_b$	30.0	57.6
60° Azimuth 75*g* Side Drop	External Pressure, Cold Environment	P_m	7.6	44.8
		$P_m + P_b$	24.7	57.6
	Internal Pressure, Hot Environment	P_m	12.9	44.8
		$P_m + P_b$	30.0	57.6
90° Azimuth 75*g* Side Drop	External Pressure, Cold Environment	P_m	8.3	44.8
		$P_m + P_b$	22.0	57.6
	Internal Pressure, Hot Environment	P_m	13.6	44.8
		$P_m + P_b$	27.2	57.6
180° Azimuth 75*g* Side Drop	External Pressure, Cold Environment	P_m	8.7	44.8
		$P_m + P_b$	24.9	57.6
	Internal Pressure, Hot Environment	P_m	13.9	44.8
		$P_m + P_b$	30.1	57.6

*The stress intensities (membrane + bending) generated in the canister during the end drop events are conservatively compared with the membrane allowable stress, P_m for SA-240, Type 304.

Figure 2.10.3-1
Basket Cross Section Finite Element Model

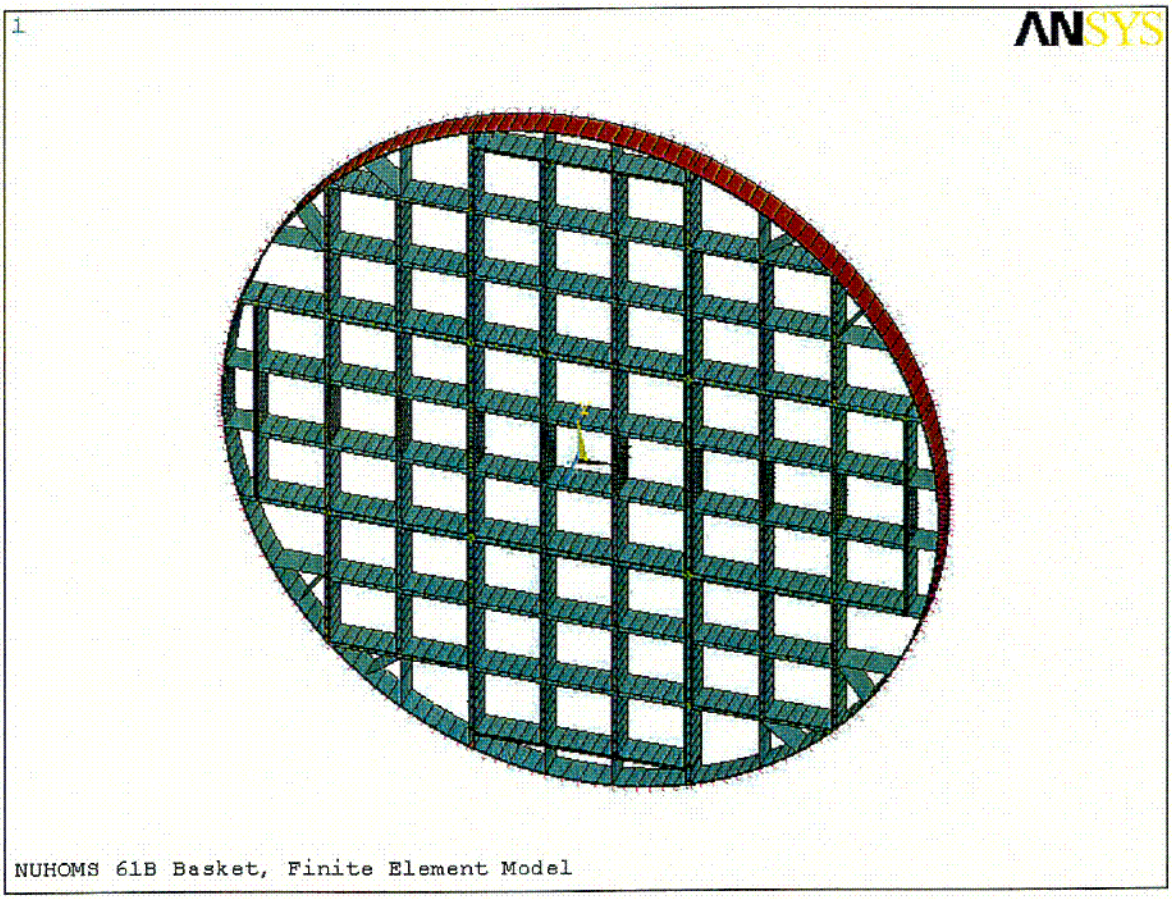

C01

Figure 2.10.3-2
Basket Cross Section Finite Element Model – Fuel Compartments

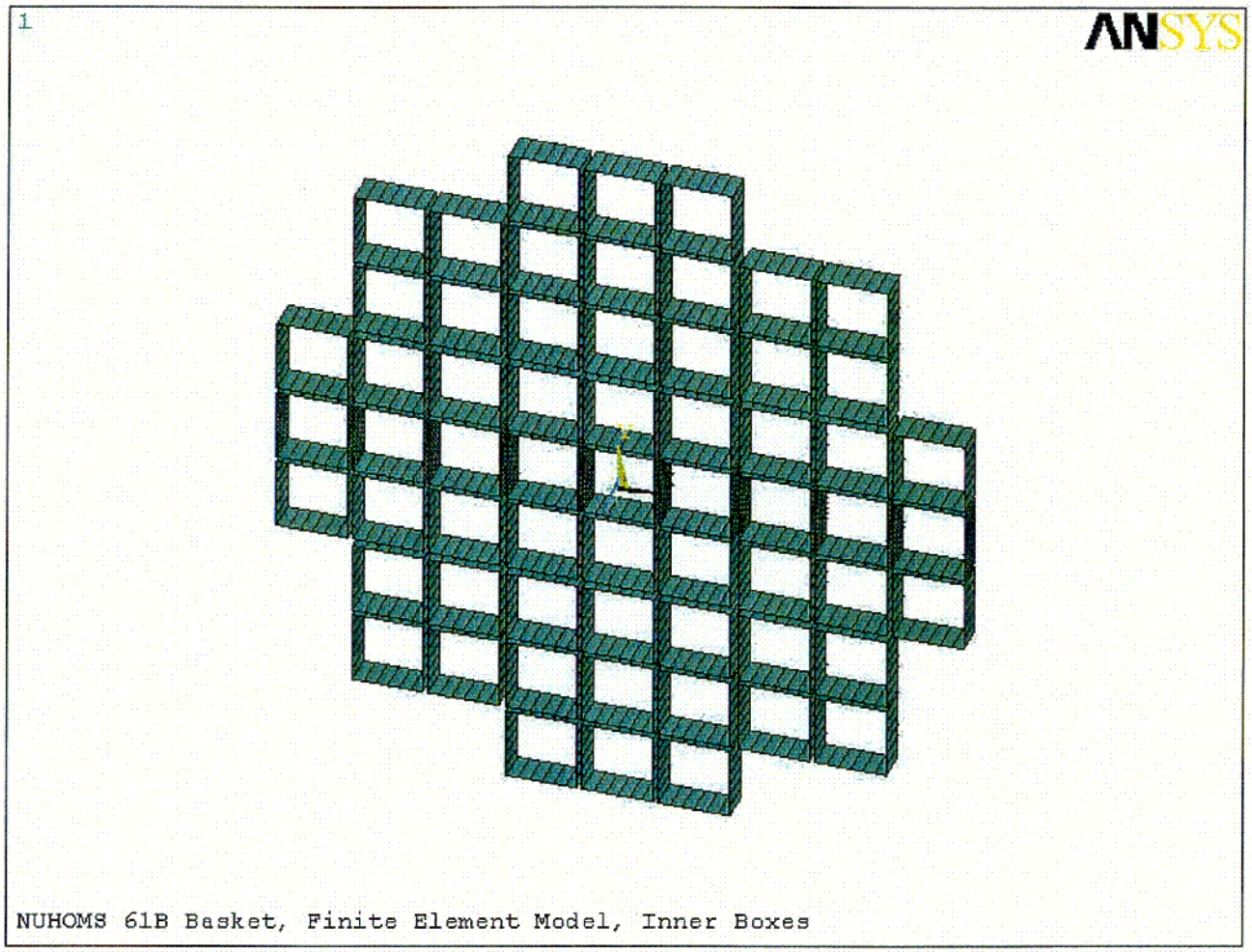

C02

Figure 2.10.3-3
Basket Cross Section Finite Element Model – Outer Wrap

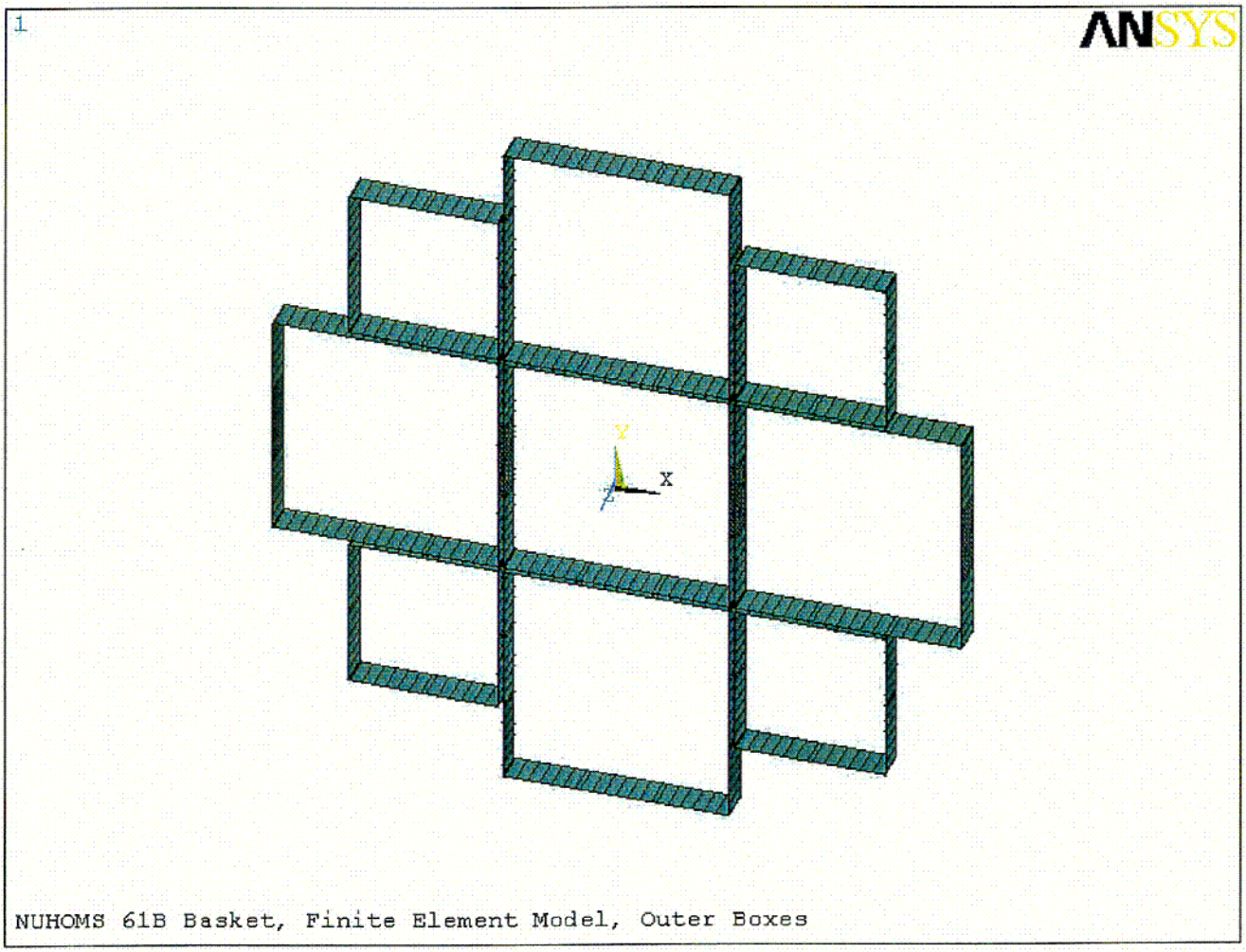

C03

Figure 2.10.3-4
Basket Cross Section Finite Element Model – Support Rails

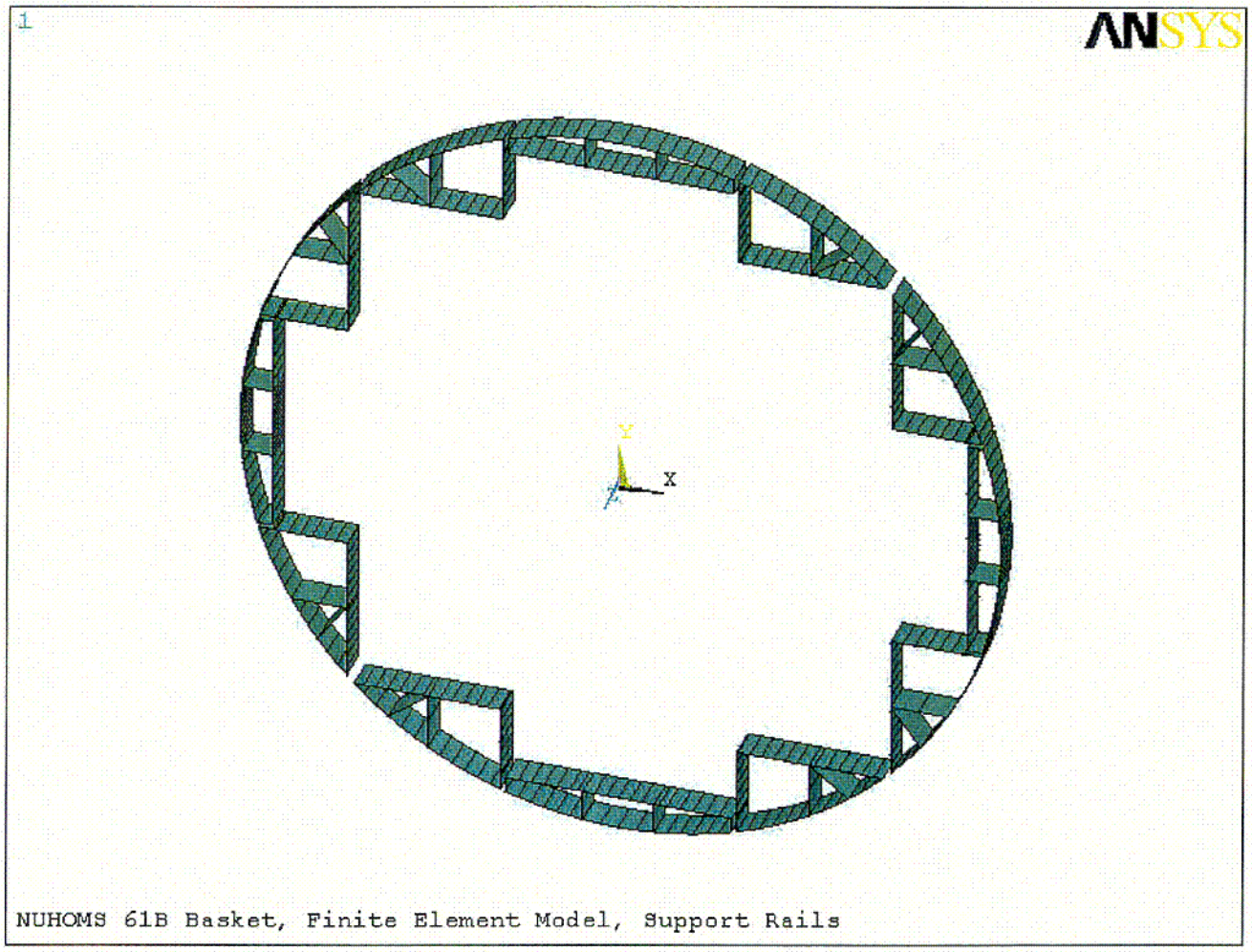

C04

Figure 2.10.3-5
Basket Side Drop Orientations

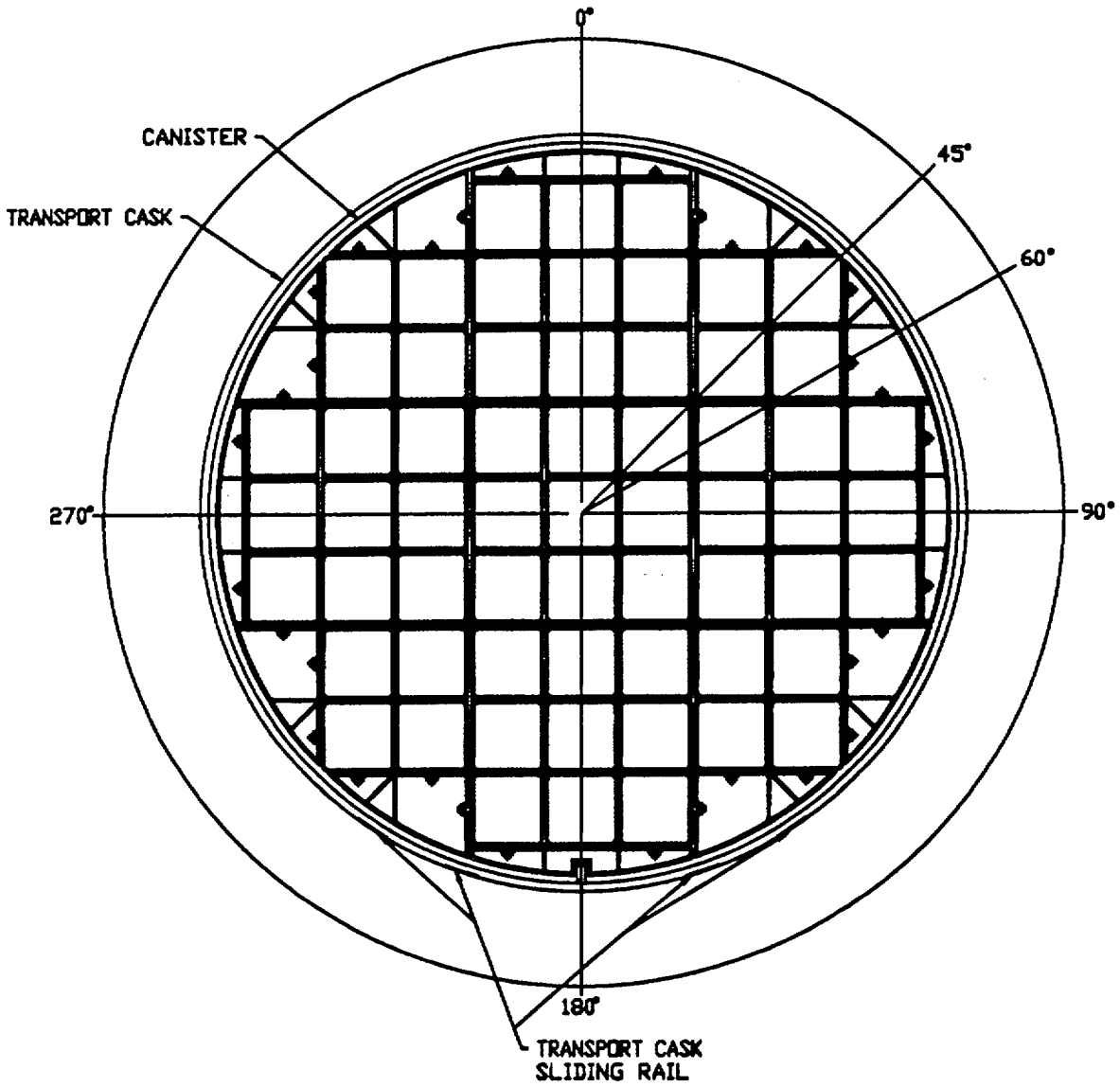

Figure 2.10.3-6
Gap Sizes between Basket Rails and Canister Inner Surface

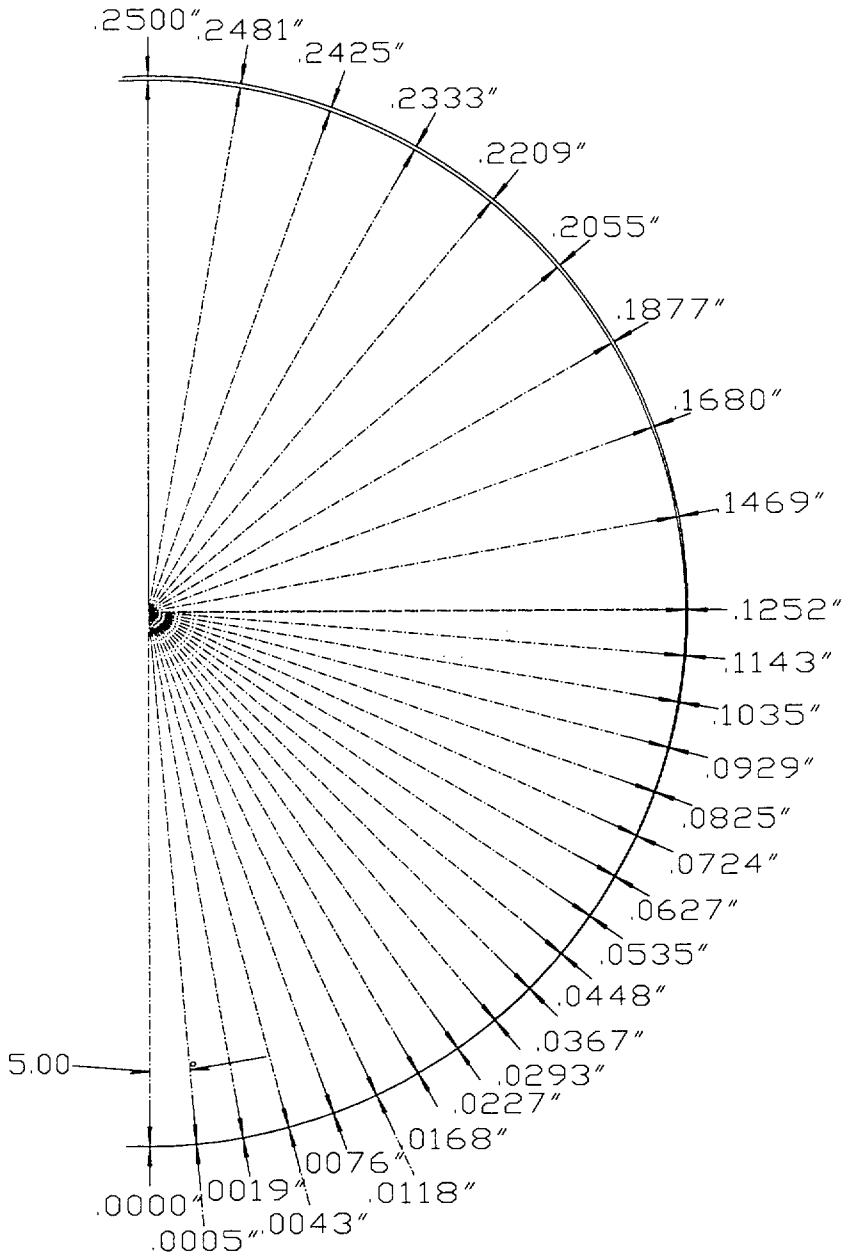

Figure 2.10.3-7
Gap Sizes between Canister Outer Surface and Transport Cask Inner Surface

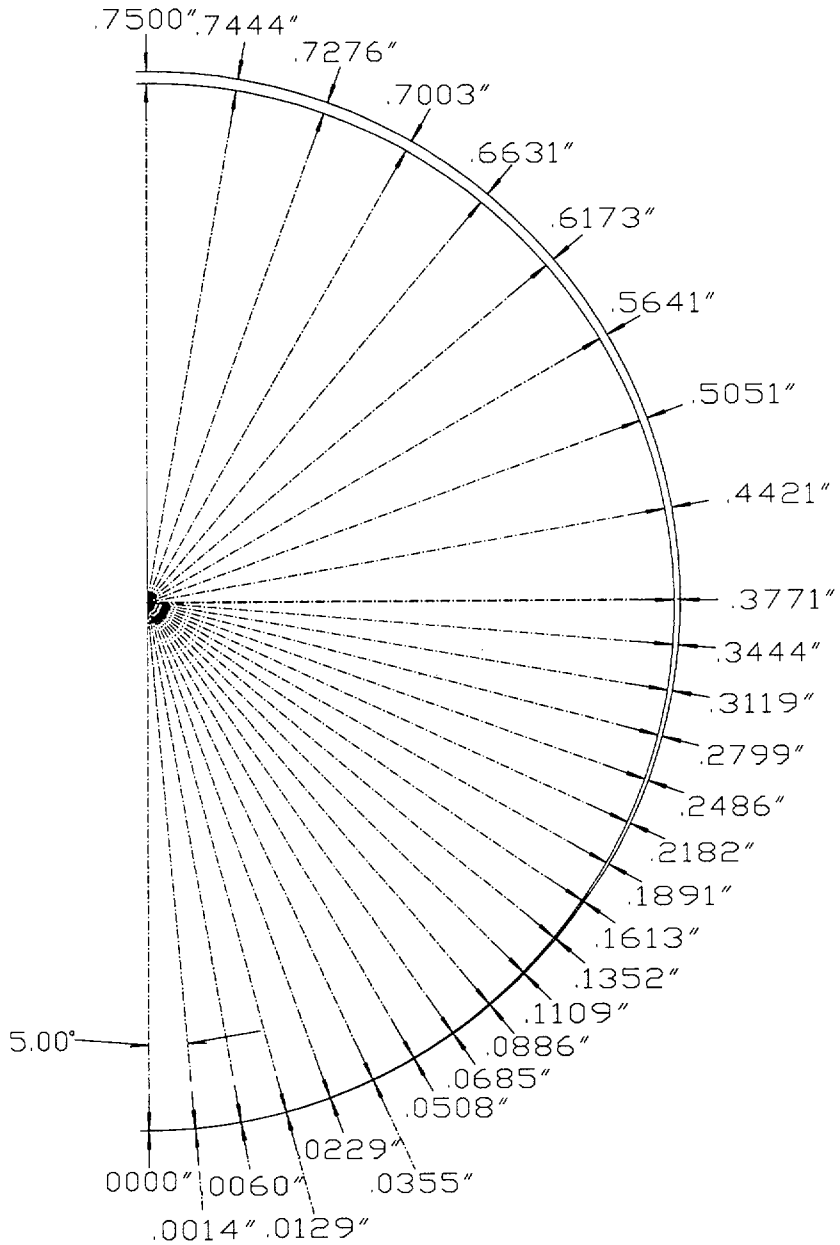

Figure 2.10.3-8
Finite Element Model – Canister & Gap Elements

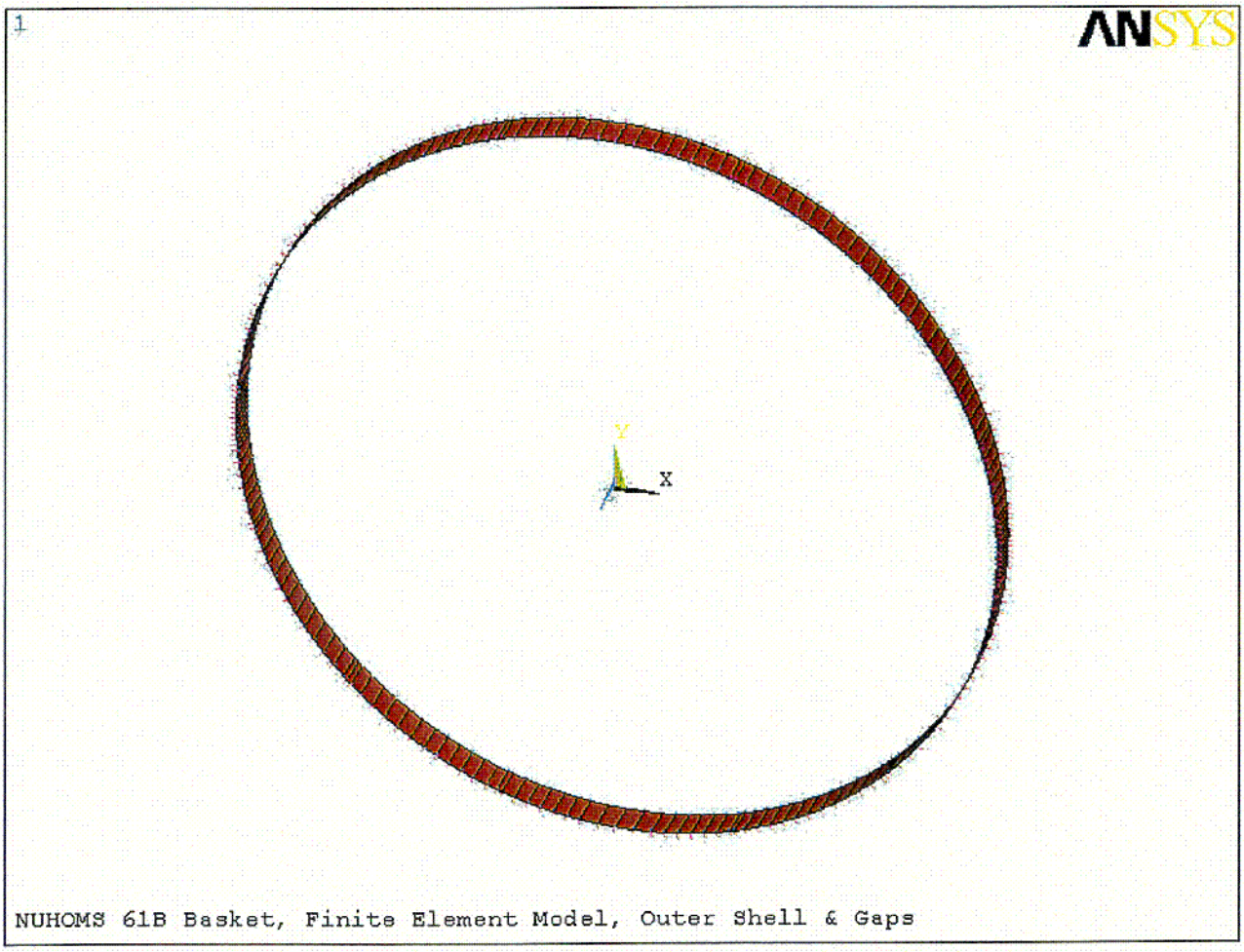

C05

Figure 2.10.3-9
Finite Element Model – Canister & Gap Elements, Enlarged View

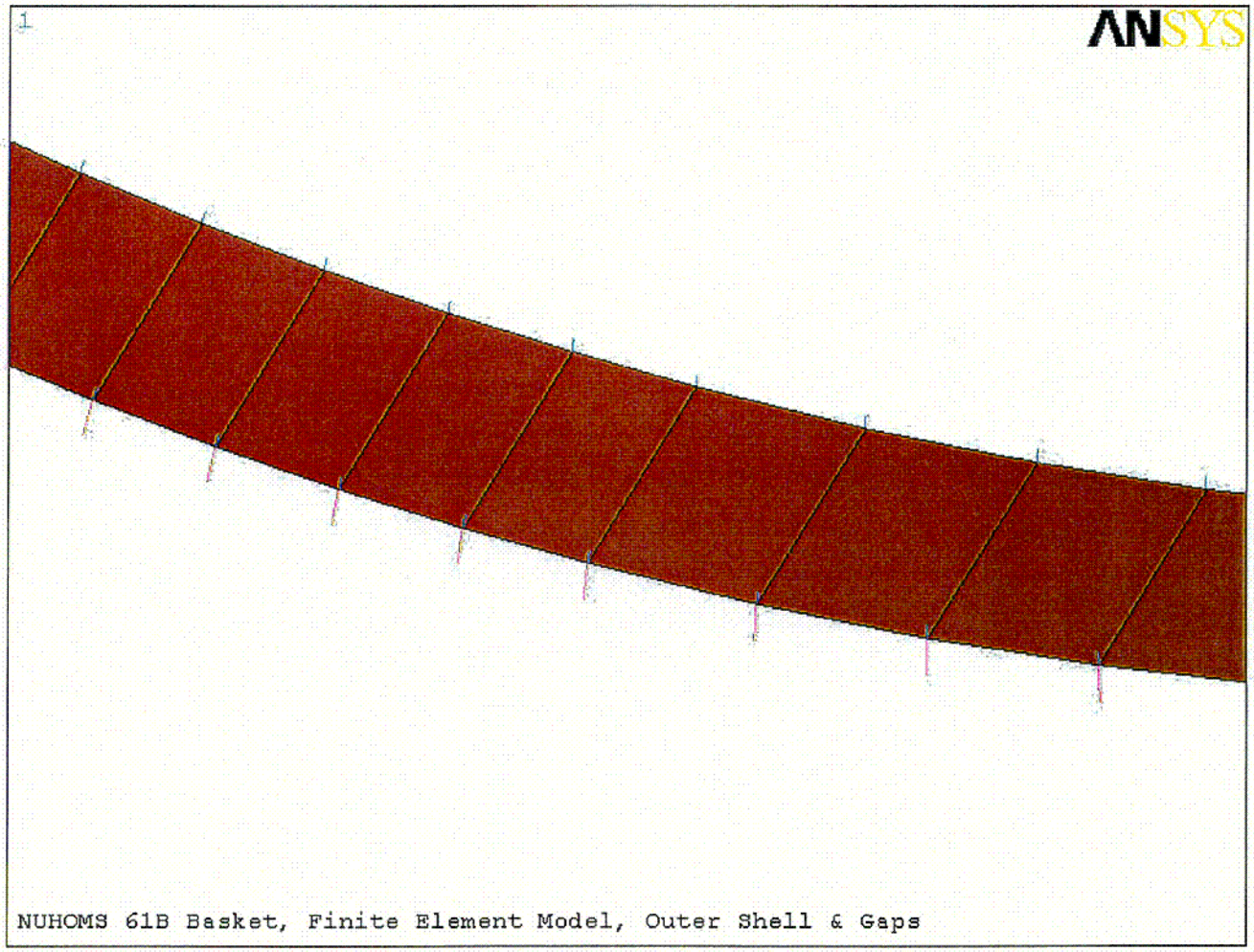

C 06

Figure 2.10.3-10
Basket Temperature Distribution at the Middle Section

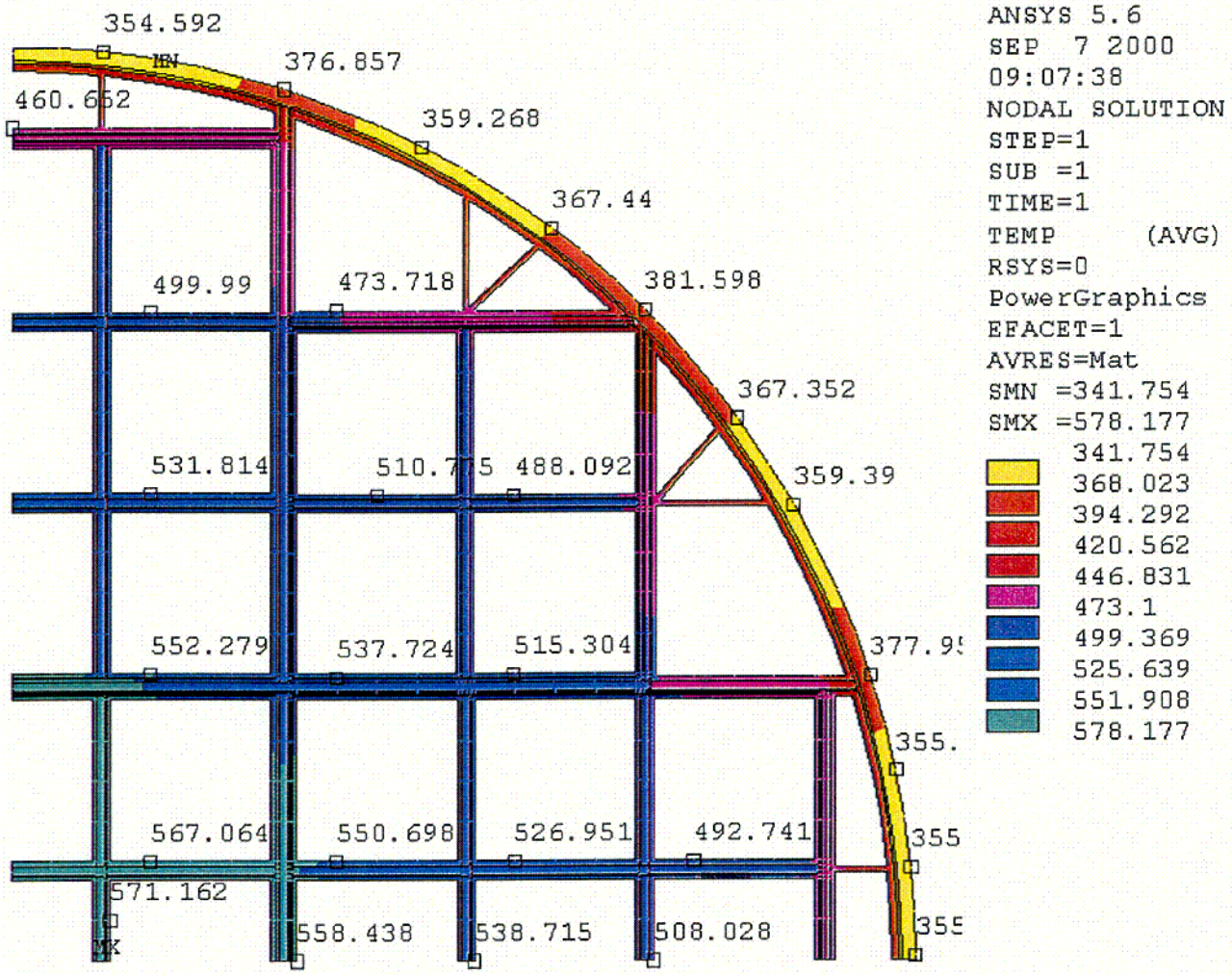

Hottest Cross-Section

C07

Figure 2.10.3-11
Basket Temperature Distribution at the Top Section

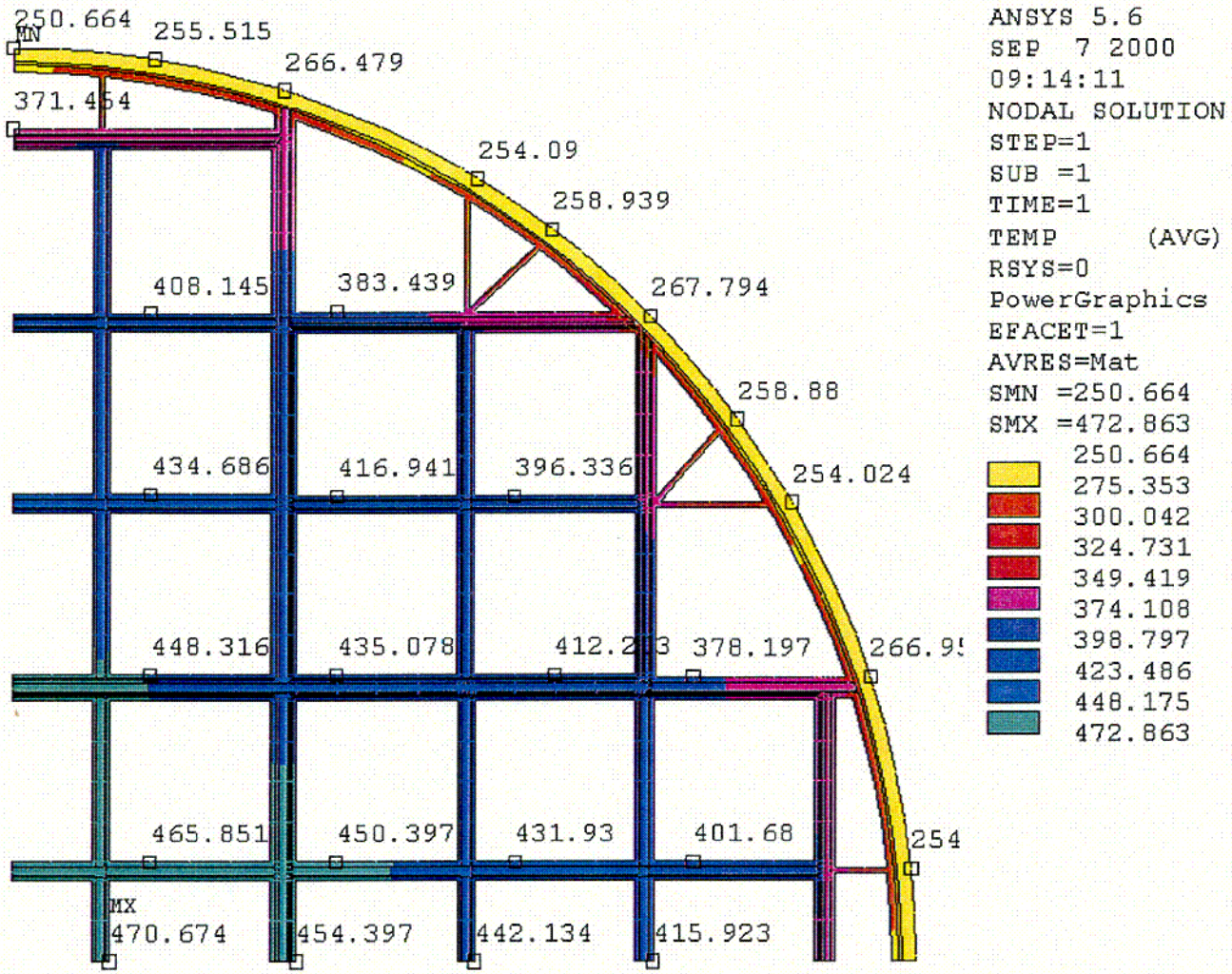

Top Cross-Section

C08

Figure 2.10.3-12
Basket Temperature Distribution at the Bottom Section

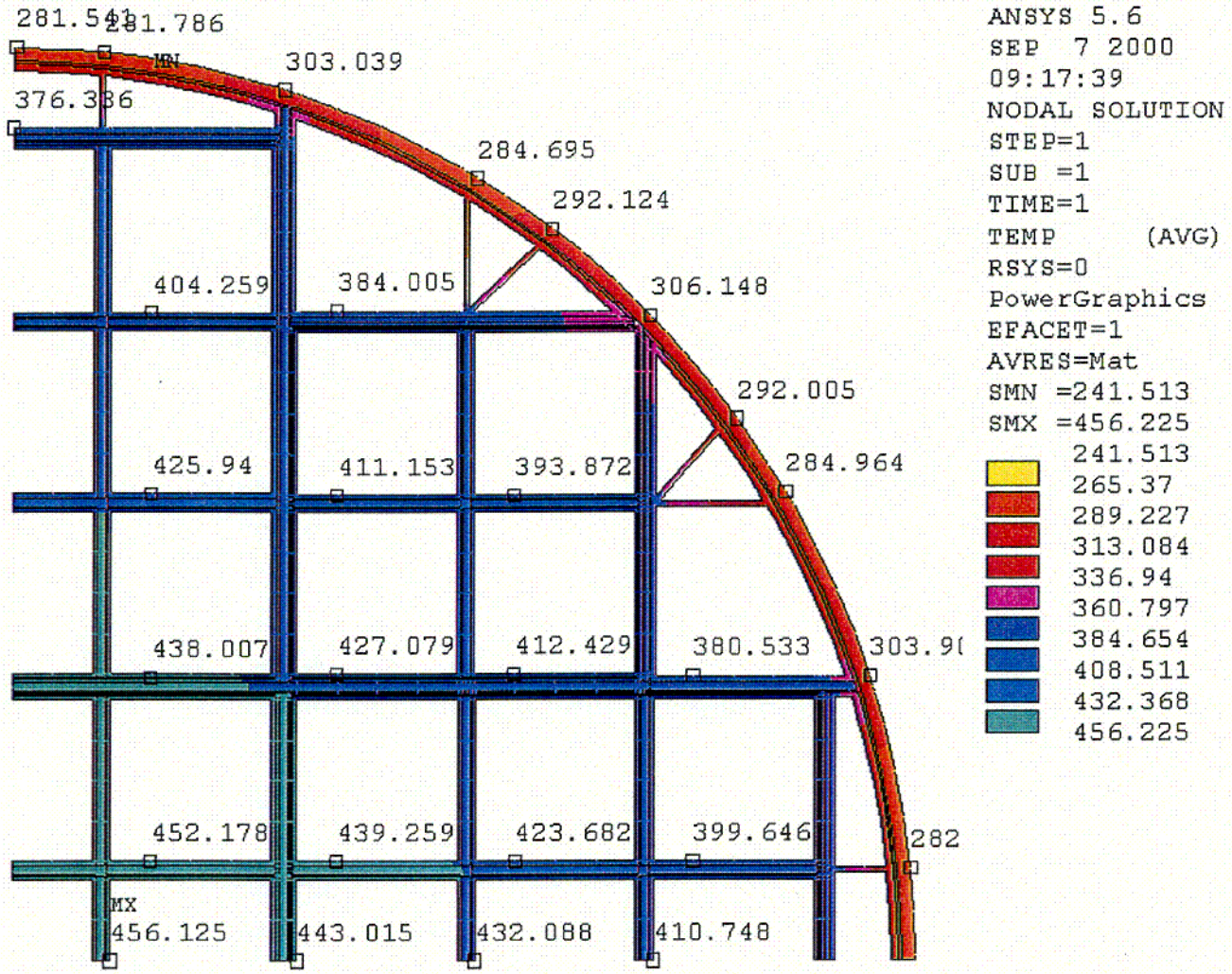

Bottom Cross-Section

C09

Figure 2.10.3-13
Basket ¼ Section Finite Element Model for Thermal Stress Analysis

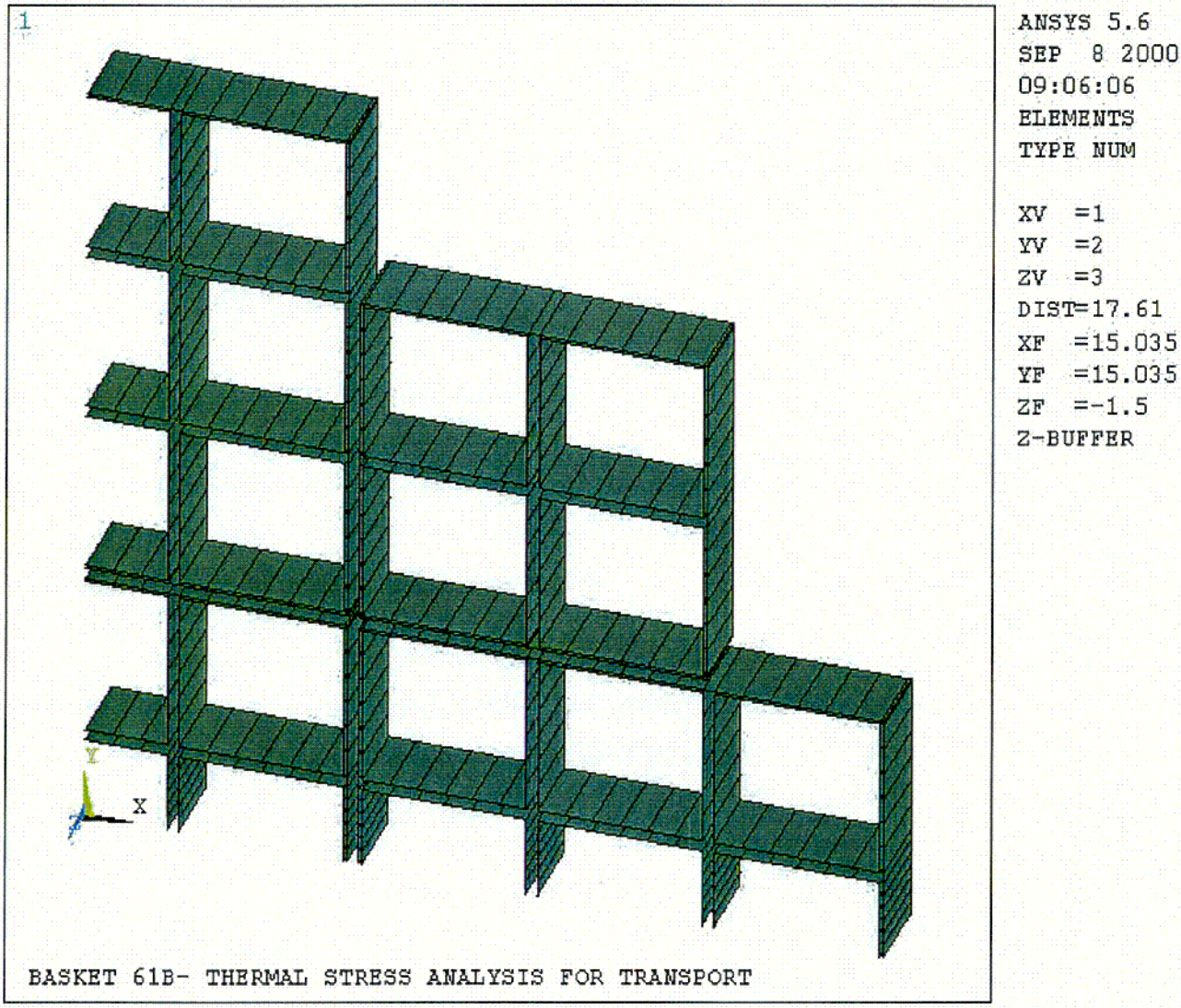

C10

Figure 2.10.3-14
Basket ¼ Section Finite Element Model with Nodal Couplings and Boundary Conditions

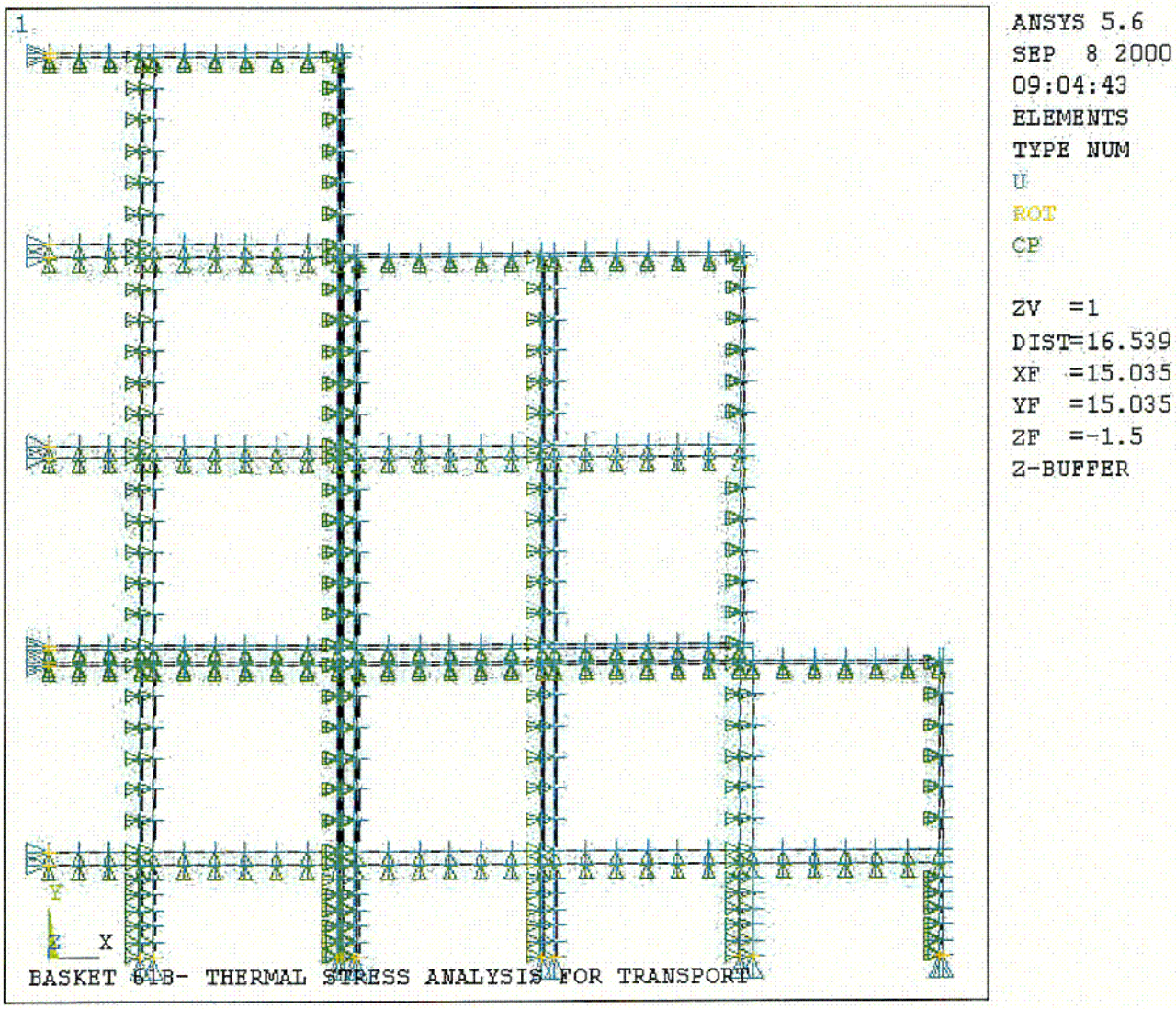

C11

Figure 2.10.3-15
Thermal Stress Analysis Geometry

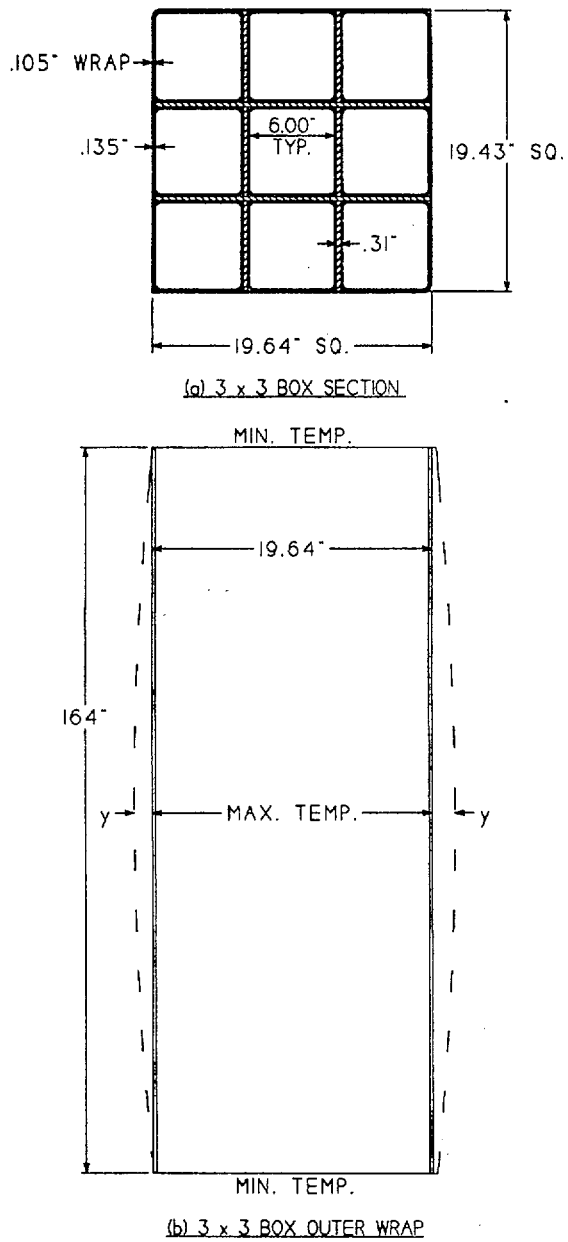

Figure 2.10.3-16
Support Rail Temperature Distribution at the Middle Section

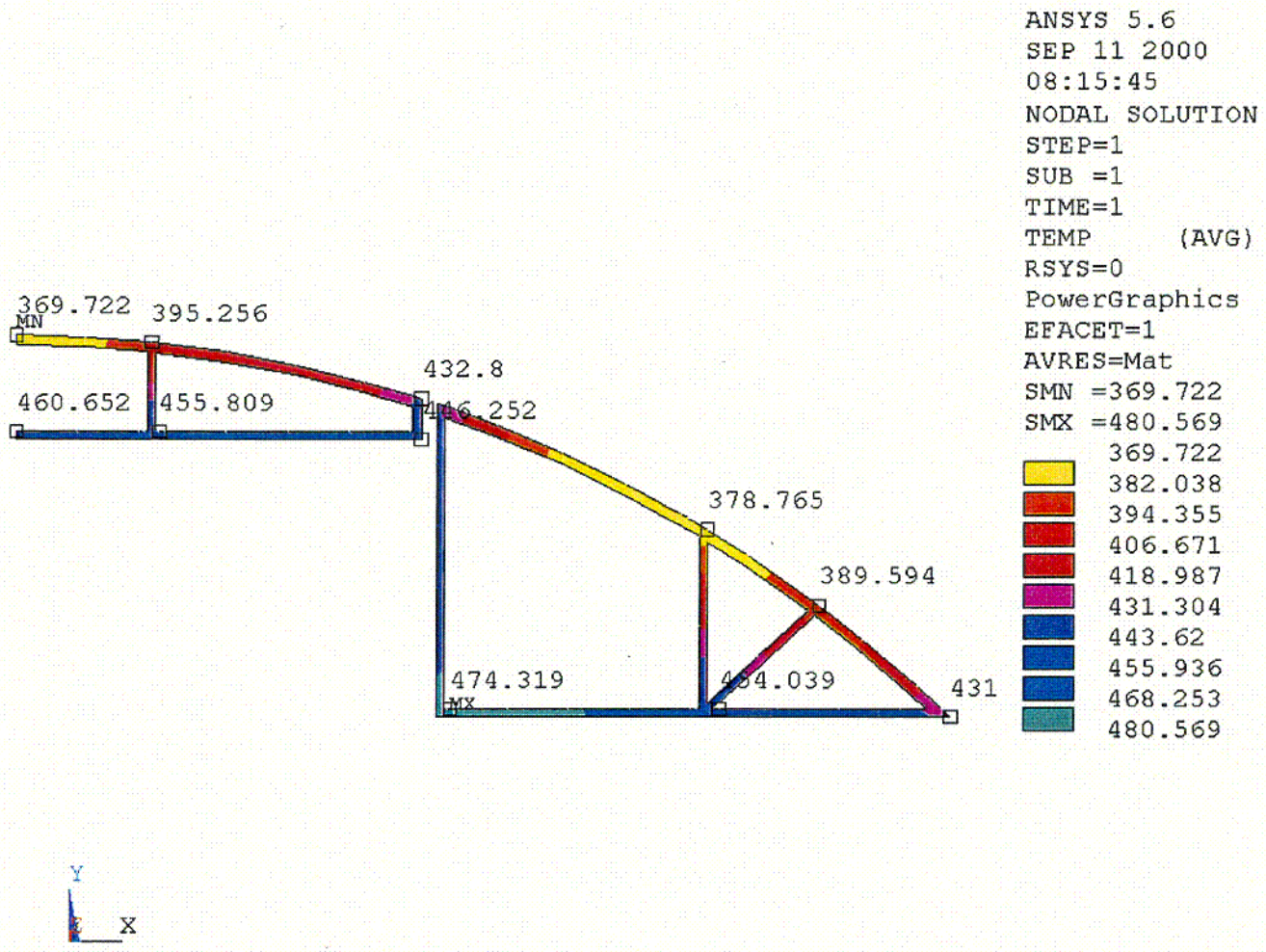

Hottest Cross-Section

C12

Figure 2.10.3-17
Support Rail Temperature Distribution at the Top Section

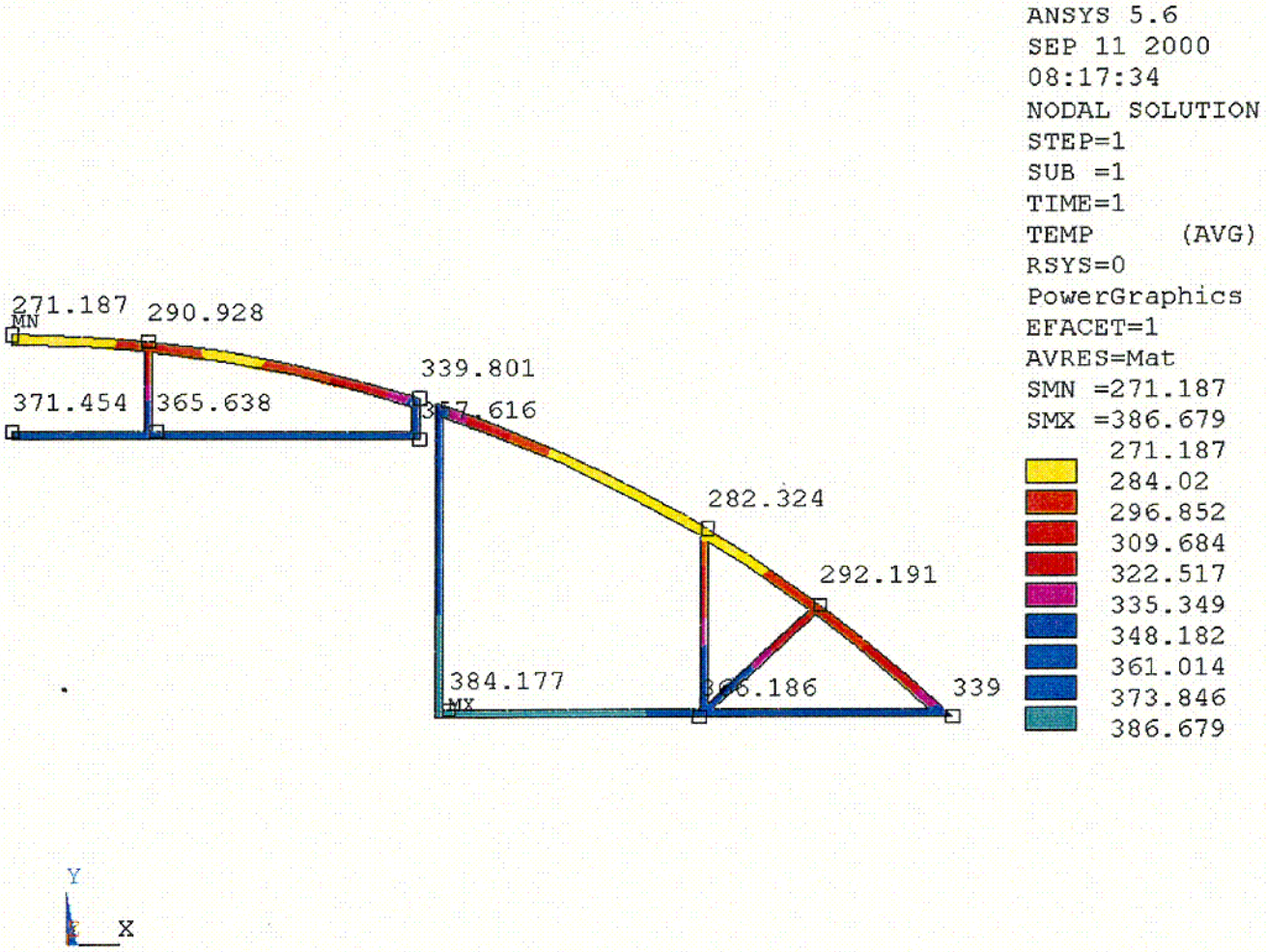

Top Cross-Section

C13

Figure 2.10.3-18
Support Rail Temperature Distribution at the Bottom Section

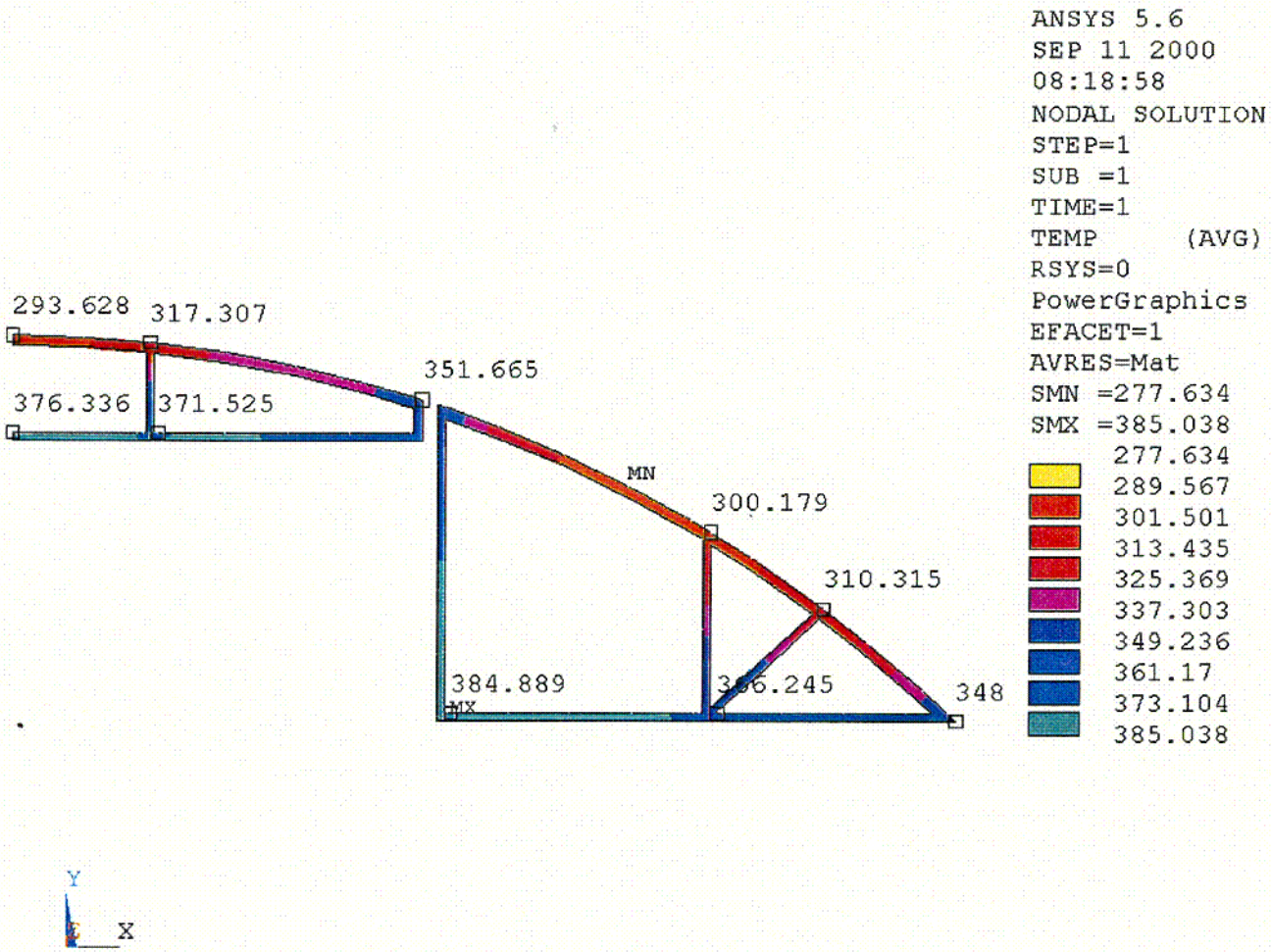

Bottom Cross-Section

C14

Figure 2.10.3-19
Basket Rail Type 1 Finite Element Model

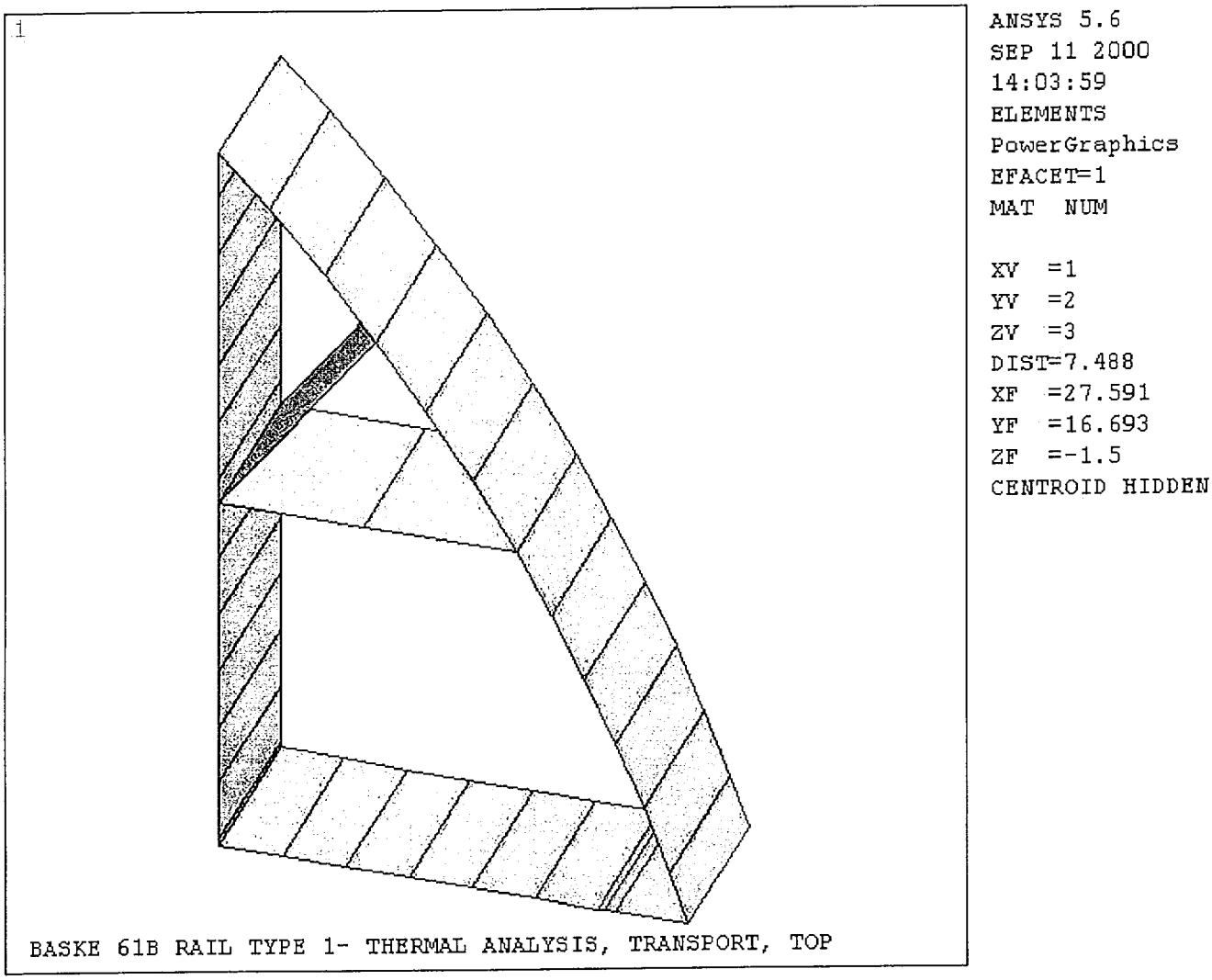

Figure 2.10.3-20
Basket Rail Type 2 Finite Element Model

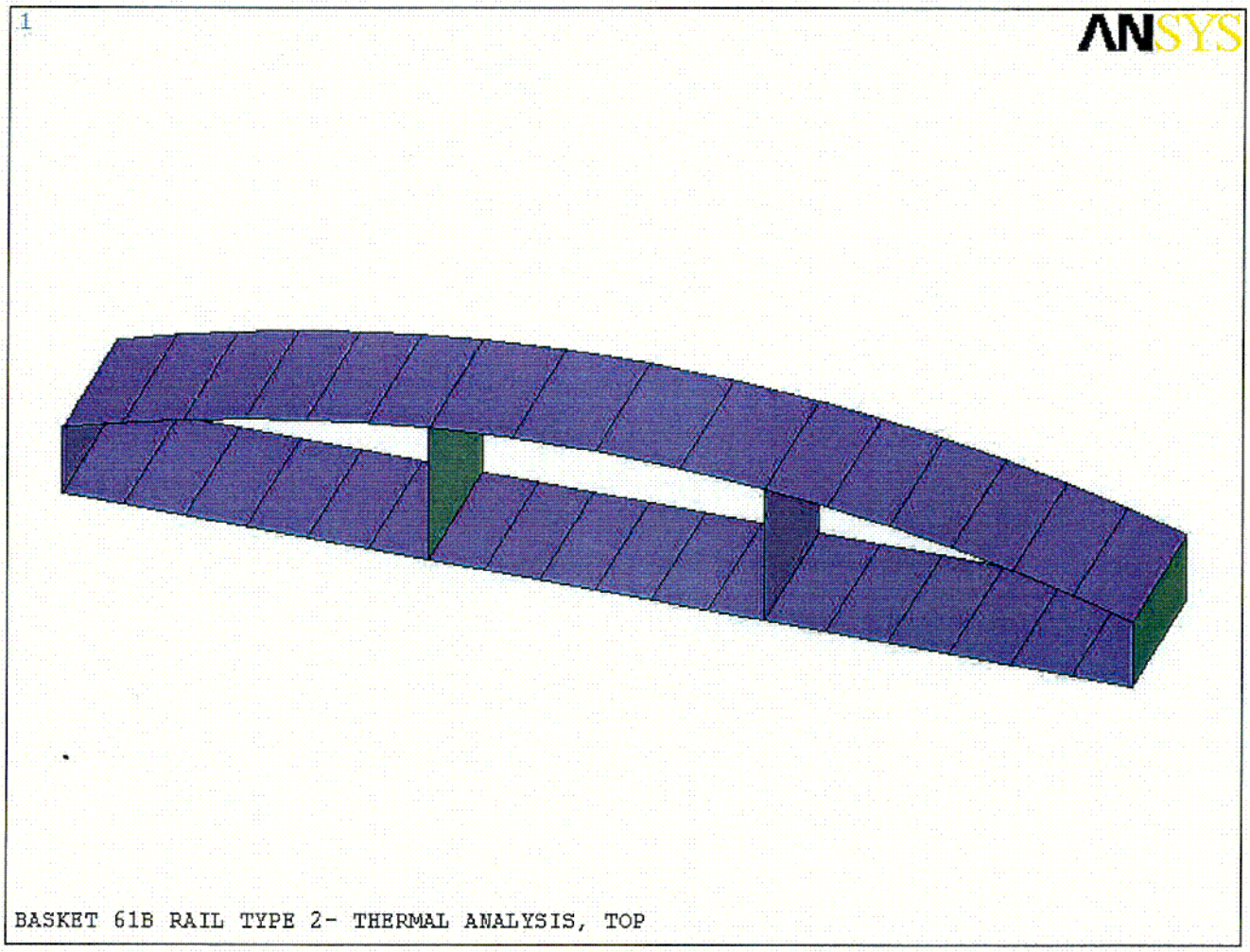

C15

Figure 2.10.3-21
45° Orientation Side Drop – Loading Condition

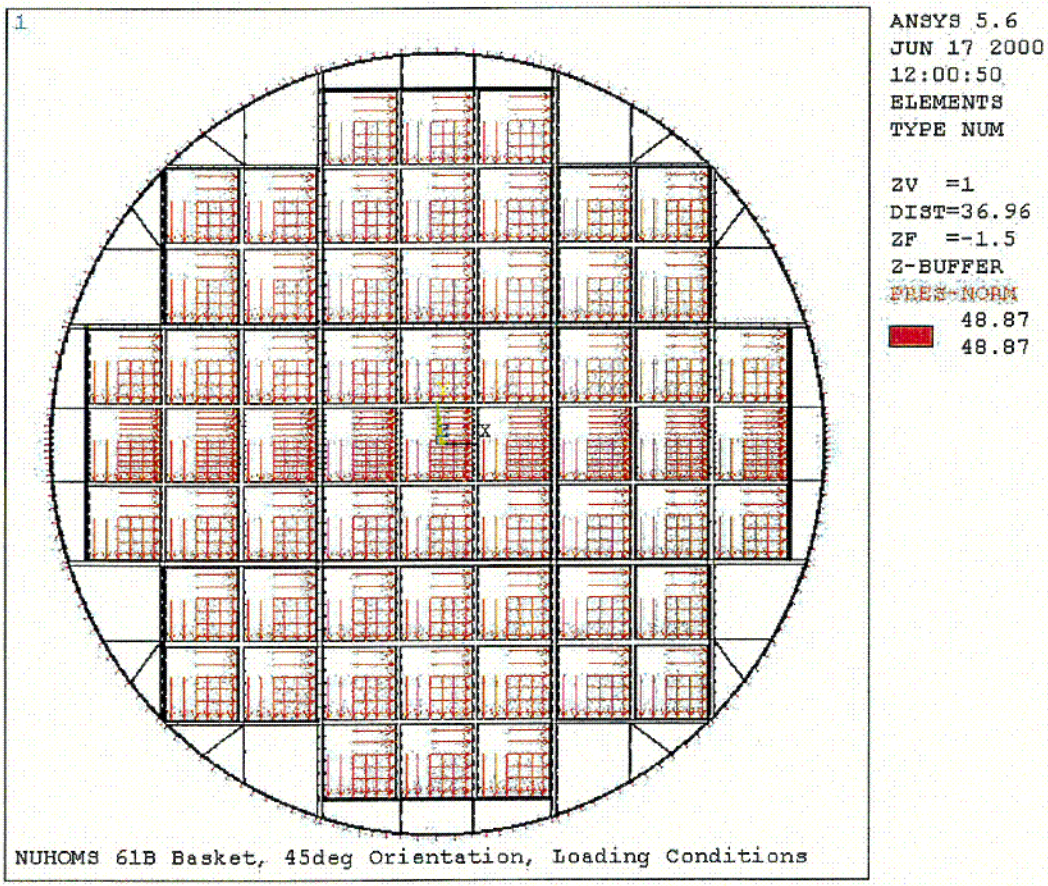

C16

Figure 2.10.3-22
60° Orientation Side Drop – Loading Condition

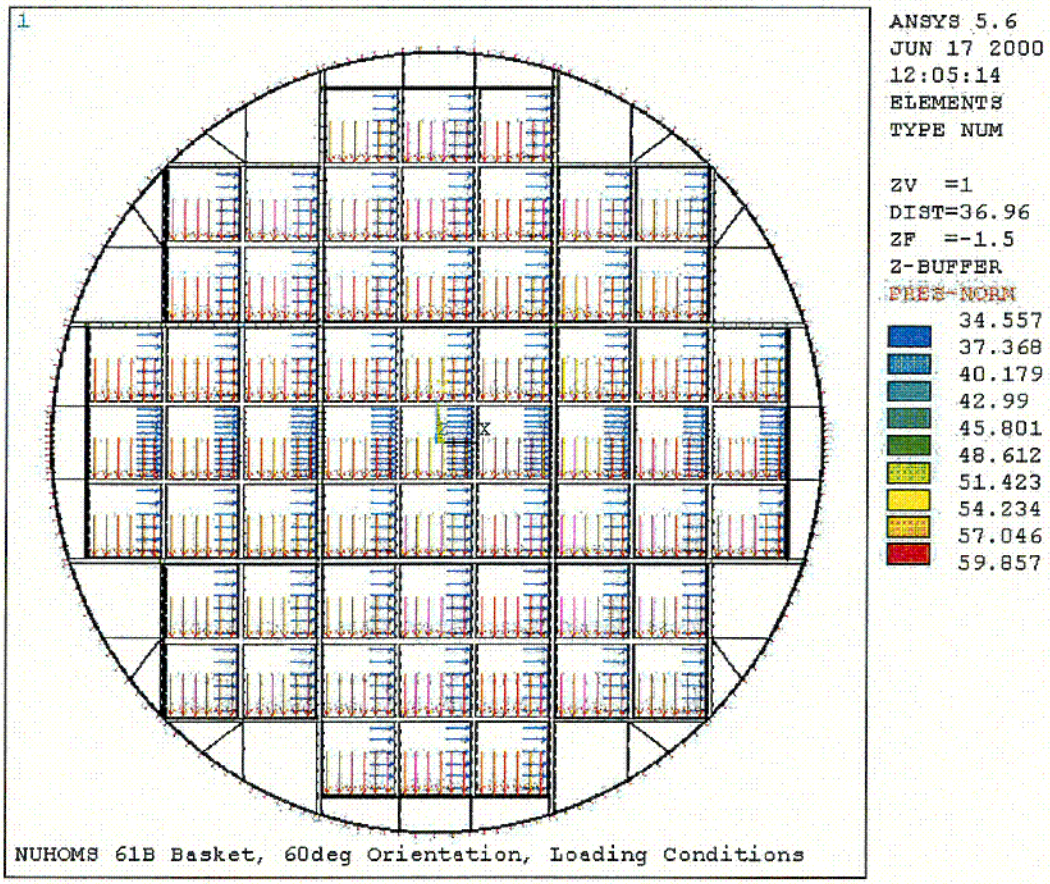

C17

Figure 2.10.3-23
90° and 180° Orientation Side Drop – Loading Condition

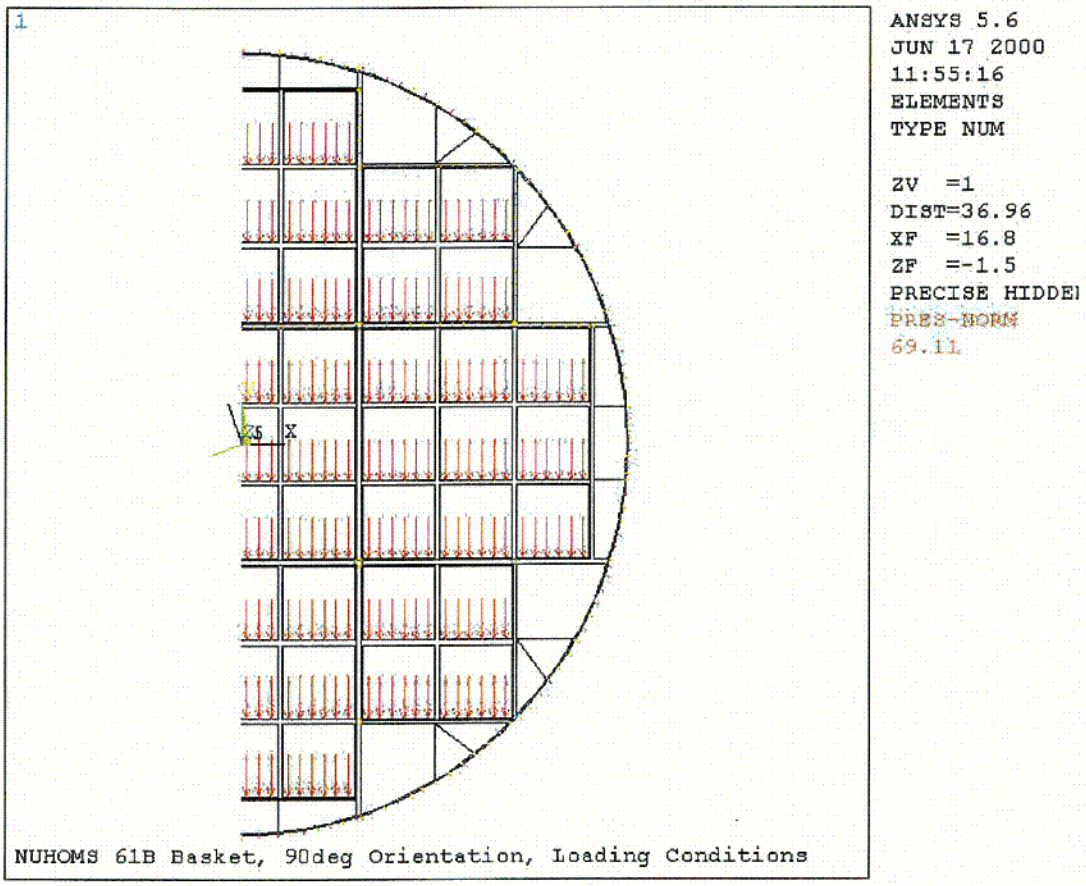

C18

Figure 2.10.3-24
45° Orientation Side Drop – Basket, P_m (75.5g)

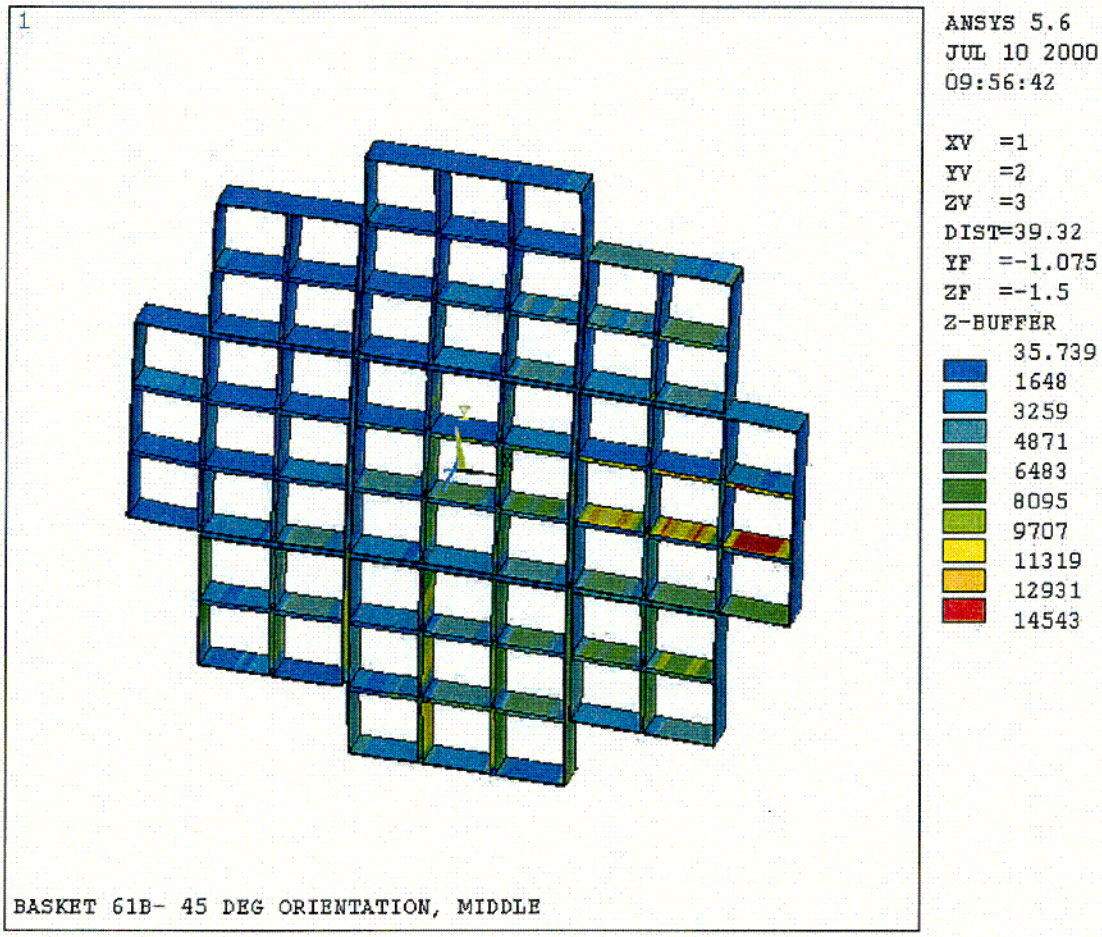

C19

Figure 2.10.3-25
45° Orientation Side Drop – Basket, $P_m + P_b$ (75.5g)

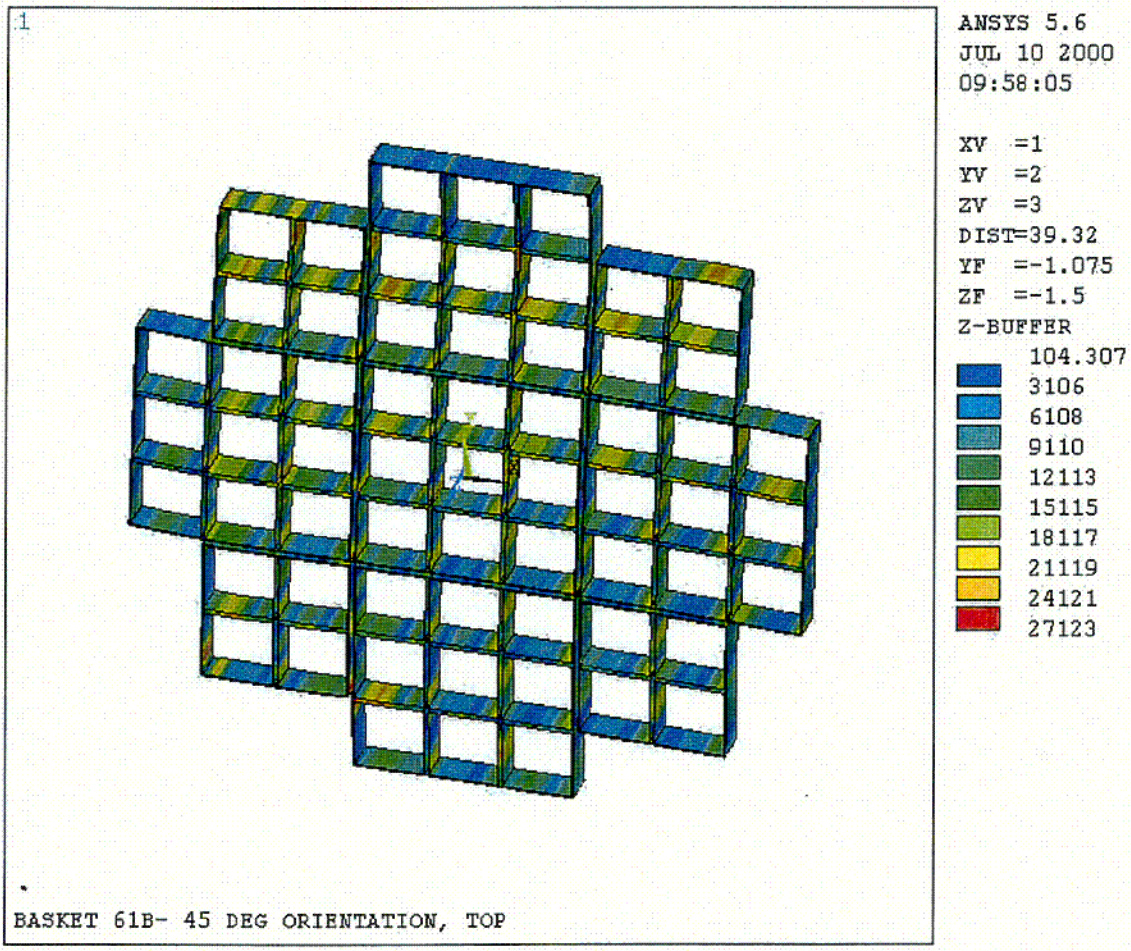

C20

Figure 2.10.3-26
45° Orientation Side Drop – Rails, P_m (75.5g)

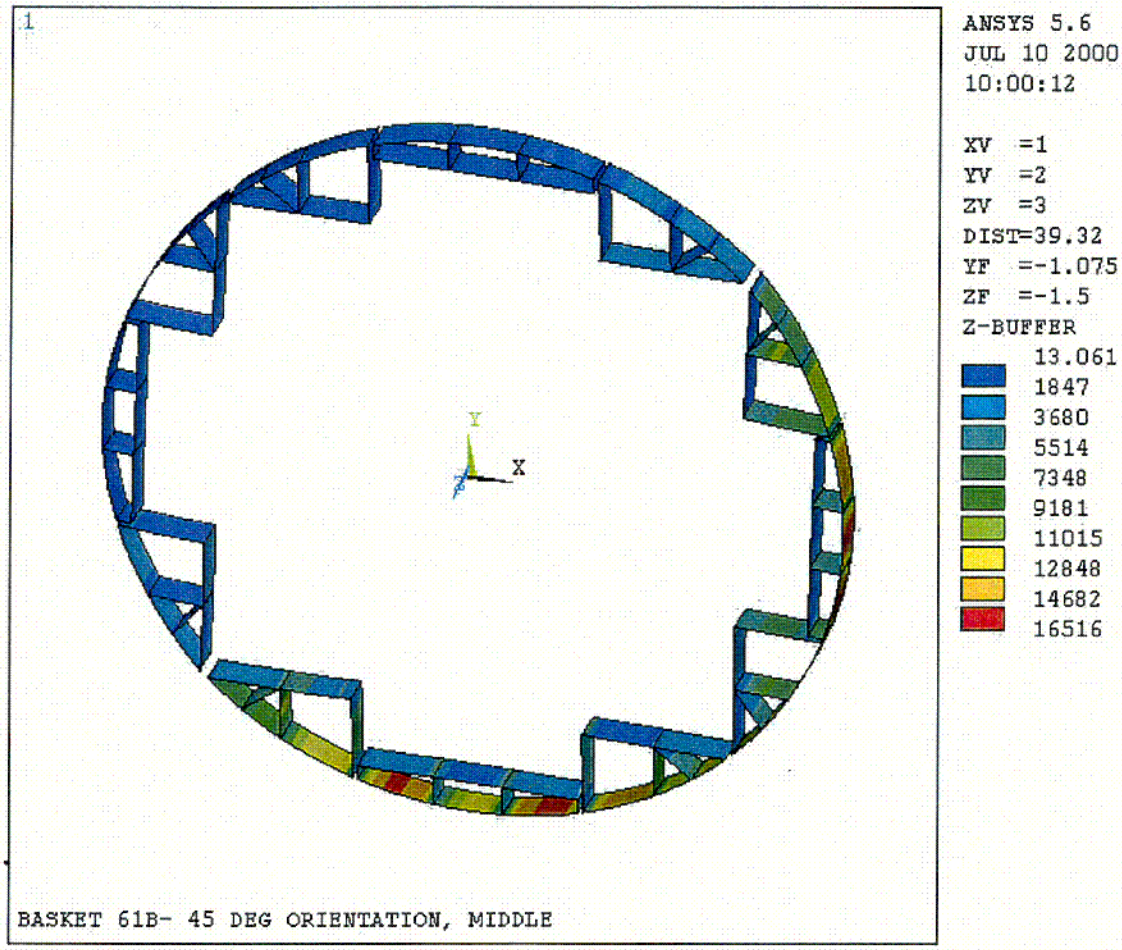

C21

Figure 2.10.3-27
45° Orientation Side Drop – Rails, $P_m + P_b$ (75.5g)

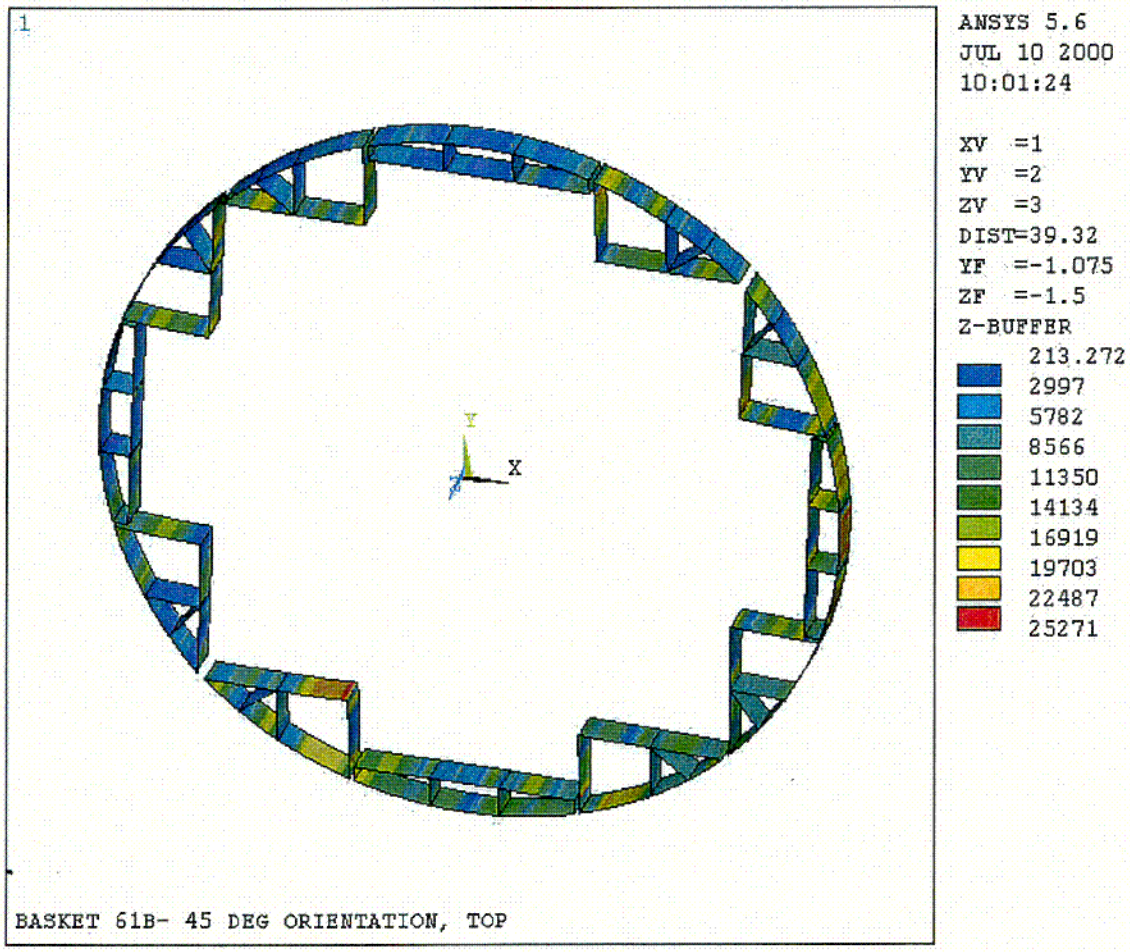

C22

Figure 2.10.3-28
60° Orientation Side Drop – Basket, P_m (75.5g)

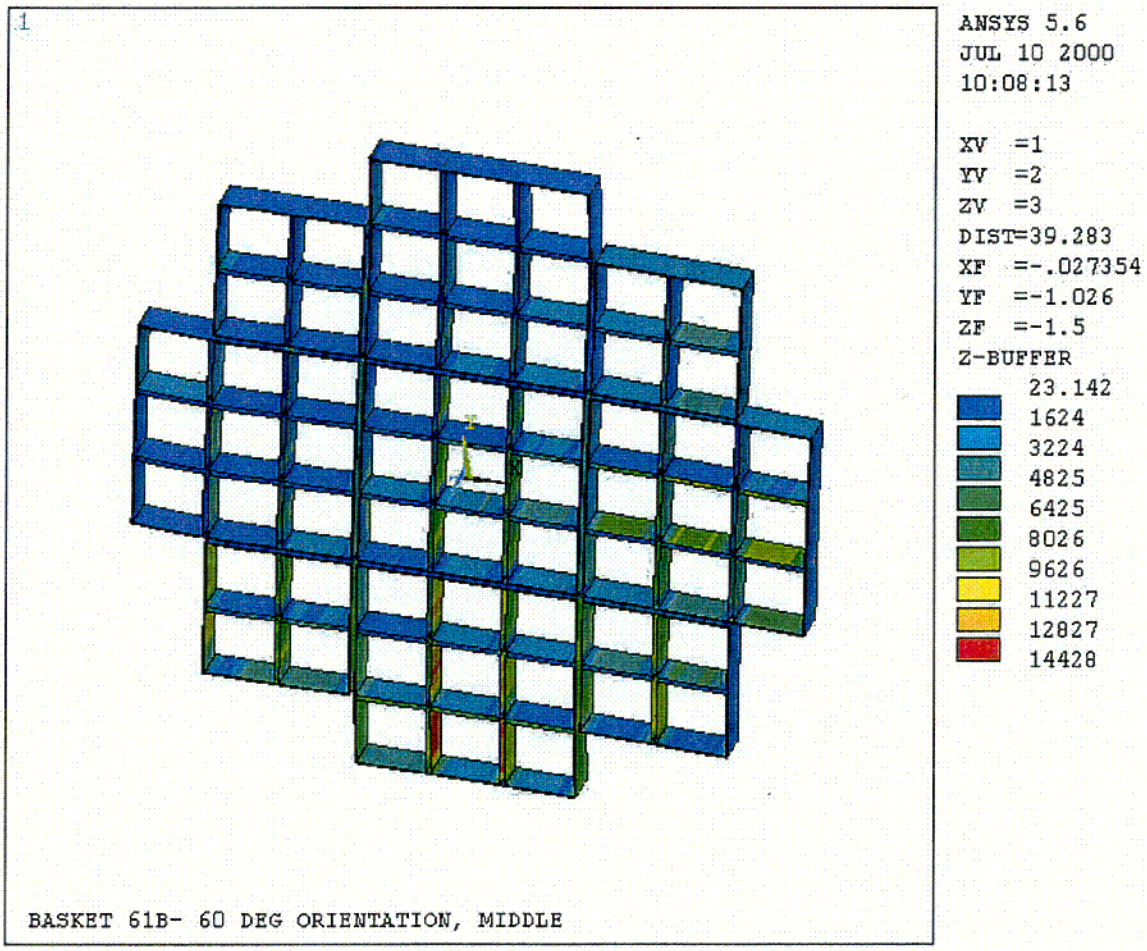

C23

Figure 2.10.3-29
60° Orientation Side Drop – Basket, $P_m + P_b$ (75.5g)

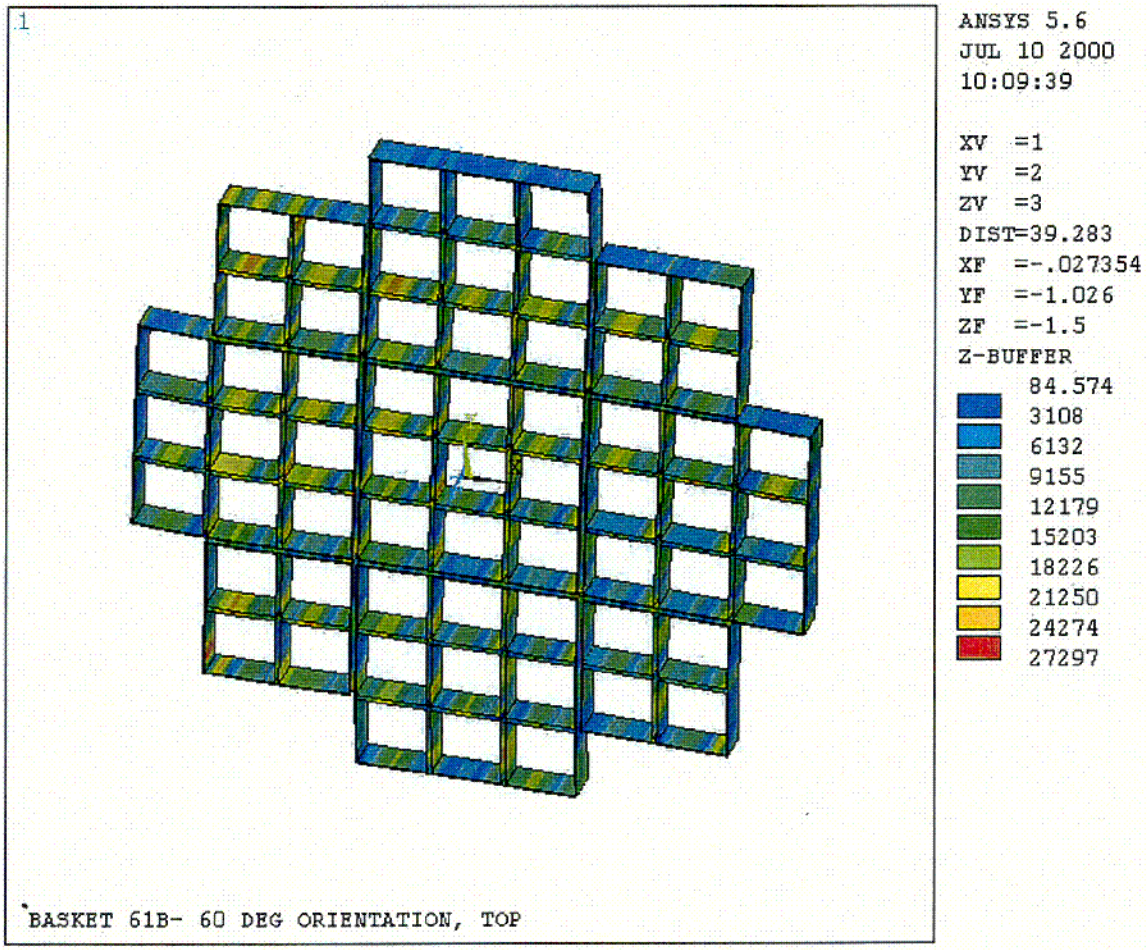

C24

Figure 2.10.3-30
60° Orientation Side Drop – Rails, P_m (75.5g)

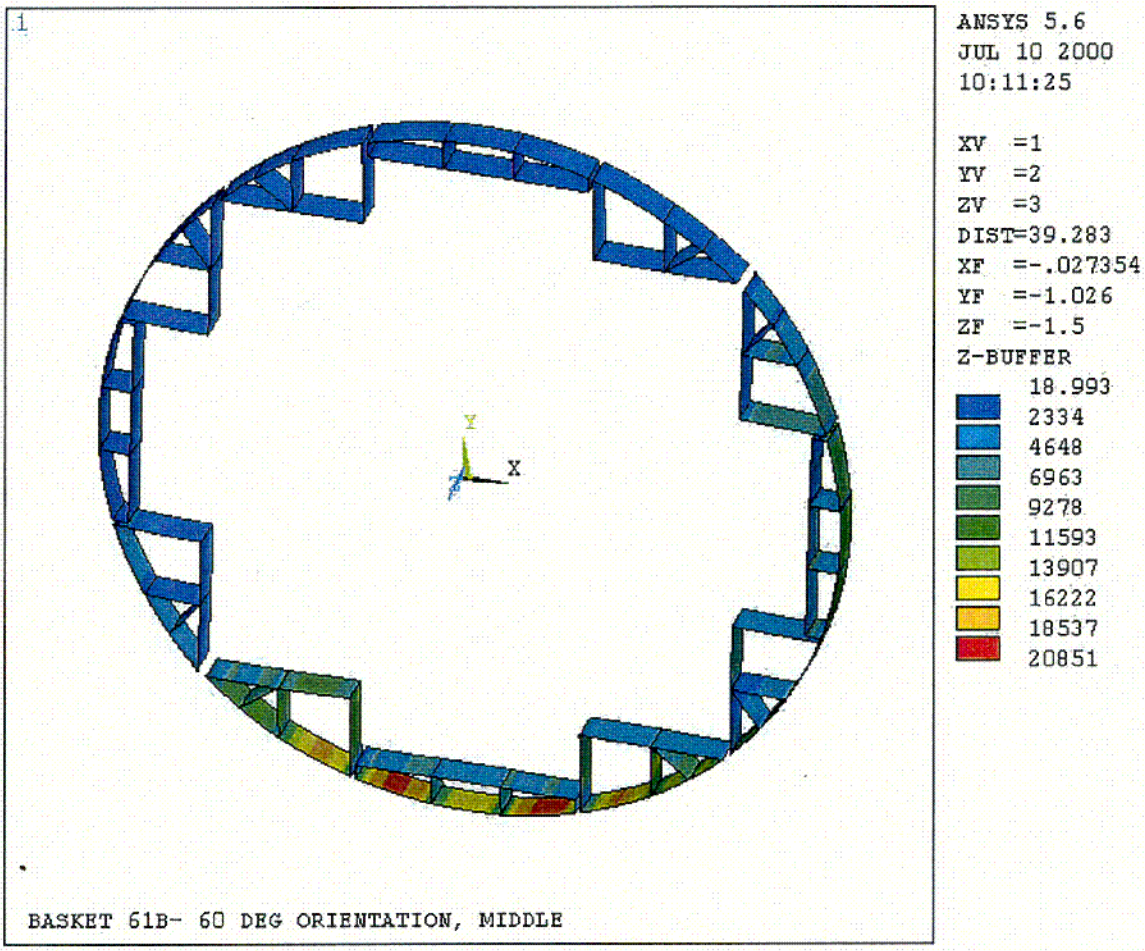

C25